

การสังเคราะห์วัสดุไฮบริดของท่อนาโนคาร์บอน/แกรไฟีน โดยใช้ตัวเร่งปฏิกิริยาผสมของเหล็ก
ออกไซด์/แกรไฟีน

นายอุกฤษณ์ ทองอนันต์กุล

จุฬาลงกรณ์มหาวิทยาลัย
CHULALONGKORN UNIVERSITY

บทคัดย่อและแฟ้มข้อมูลฉบับเต็มของวิทยานิพนธ์ตั้งแต่ปีการศึกษา 2554 ที่ให้บริการในคลังปัญญาจุฬาฯ (CUIR)
เป็นแฟ้มข้อมูลของนิสิตเจ้าของวิทยานิพนธ์ ที่ส่งผ่านทางบัณฑิตวิทยาลัย

The abstract and full text of theses from the academic year 2011 in Chulalongkorn University Intellectual Repository (CUIR)
are the thesis authors' files submitted through the University Graduate School.

วิทยานิพนธ์นี้เป็นส่วนหนึ่งของการศึกษาตามหลักสูตรปริญญาวิศวกรรมศาสตรมหาบัณฑิต

สาขาวิชาวิศวกรรมเคมี ภาควิชาวิศวกรรมเคมี

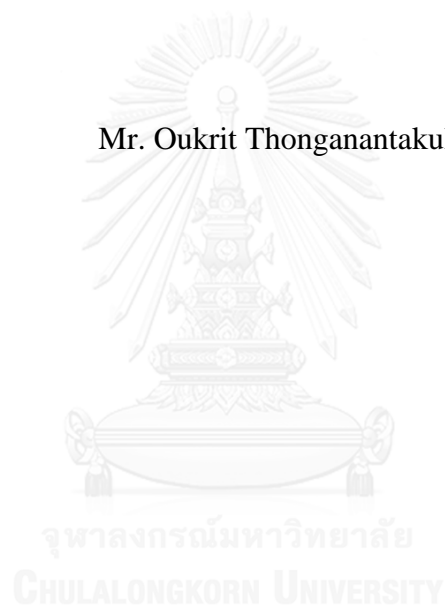
คณะวิศวกรรมศาสตร์ จุฬาลงกรณ์มหาวิทยาลัย

ปีการศึกษา 2559

ลิขสิทธิ์ของจุฬาลงกรณ์มหาวิทยาลัย

Synthesis of carbon nanotube/graphene hybrid material using iron oxide/graphene
composite catalyst

Mr. Oukrit Thonganantakul



A Thesis Submitted in Partial Fulfillment of the Requirements
for the Degree of Master of Engineering Program in Chemical Engineering
Department of Chemical Engineering
Faculty of Engineering
Chulalongkorn University
Academic Year 2016
Copyright of Chulalongkorn University

อภิญญา ทองอนันตกุล : การสังเคราะห์วัสดุไฮบริดของท่อนาโนคาร์บอน/แกรฟีนโดยใช้ตัวเร่งปฏิกิริยาผสมของเหล็กออกไซด์/แกรฟีน (Synthesis of carbon nanotube/graphene hybrid material using iron oxide/graphene composite catalyst) อ.ที่ปริกษาวิทยานิพนธ์หลัก: รศ. ดร.ชัชชัย ชรินพานิชกุล, อ.ที่ปริกษาวิทยานิพนธ์ร่วม: ดร.วิรุฒิ ชัยวัฒน์, ดร.ศิริระ ศรีนิเวศน์, 68 หน้า.

การสังเคราะห์ท่อนาโนคาร์บอนบนตัวเร่งปฏิกิริยาผสมของเหล็กออกไซด์/แกรฟีนด้วยวิธีการตกตะกอนไอเชิงเคมีโดยมีเฮกเซนเป็นแหล่งคาร์บอน การวิเคราะห์คุณสมบัติของผลิตภัณฑ์ที่สังเคราะห์ขึ้นประกอบด้วยสมบัติทางด้านสัณฐานวิทยา หมู่ฟังก์ชัน และโครงสร้างด้านผลึก จากอิทธิพลของอุณหภูมิที่ 700, 800, 900, และ 1000 °C ซึ่งใช้ในการสังเคราะห์ท่อนาโนคาร์บอนพบว่า ขนาดอนุภาคเหล็กก่อนการเกิดขึ้นของท่อนาโนคาร์บอนมีขนาด 14, 72, 98, และ 119 นาโนเมตร ตามลำดับ และผลิตภัณฑ์ที่สังเคราะห์มีลักษณะทางกายภาพดังนี้ ท่อนาโนคาร์บอนมีเส้นผ่านศูนย์กลาง 20-50, 20-80 และ 50-100 นาโนเมตร, และอนุภาคคาร์บอนทรงกลมที่มีเส้นผ่านศูนย์กลาง 320-730 นาโนเมตร ตามลำดับ โดยมีข้อมูลทางด้านสัณฐานวิทยายืนยันว่า ท่อนาโนคาร์บอนที่เกิดขึ้นบนตัวเร่งปฏิกิริยาที่มีเหล็กอยู่ในเฟสแอลฟา และอุณหภูมิที่เหมาะสมที่ 900 °C และยังมีความเป็นผลึกที่สูงถึง 1.77 เปรียบเทียบกับเงื่อนไขที่อุณหภูมิ 700 และ 800 °C มีความเป็นผลึกที่ 0.76 และ 1.45 ตามลำดับ

ภายใต้อุณหภูมิที่ใช้ในการสังเคราะห์ท่อนาโนคาร์บอน พบว่าเฟสของเหล็กมีการเปลี่ยนจากแอลฟาเป็นแกมมาอย่างสมบูรณ์ที่อุณหภูมิ 1000 °C เมื่อนำไปใช้ในการสังเคราะห์ท่อนาโนคาร์บอน พบว่า มีการเกิดขึ้นของชั้นฟิล์มคาร์บอนเคลือบอนุภาคเหล็กที่อยู่ในเฟสแกมมา แสดงให้เห็นว่าท่อนาโนคาร์บอนสามารถสังเคราะห์ได้จากตัวเร่งปฏิกิริยาเหล็กที่อยู่ในเฟสแอลฟา

ภาควิชา วิศวกรรมเคมี
สาขาวิชา วิศวกรรมเคมี
ปีการศึกษา 2559

ลายมือชื่อนิสิต

ลายมือชื่อ อ.ที่ปริกษาหลัก

ลายมือชื่อ อ.ที่ปริกษาร่วม

ลายมือชื่อ อ.ที่ปริกษาร่วม

5870373721 : MAJOR CHEMICAL ENGINEERING

KEYWORDS: CARBON NANOTUBES / IRON OXIDE/GRAPHENE OXIDE COMPOSITE
/ CARBON NANOTUBE/GRAPHENE MATERIALS / ALPHA IRON

OUKRIT THONGANANTAKUL: Synthesis of carbon nanotube/graphene hybrid material using iron oxide/graphene composite catalyst. ADVISOR: ASSOC. PROF. TAWATCHAI CHARINPANITKUL, D.Eng., CO-ADVISOR: WEERAWUT CHAIWAT, Ph.D., SIRA SRINIVES, Ph.D., 68 pp.

In this research, carbon nanotubes (CNTs) were synthesized on iron oxide/graphene oxide composites (Fe/GO) by chemical vapor deposition (CVD) with n-Hexane as the carbon source. The Fe/GO composites and the carbon nanotube/graphene (CNT/G) hybrid materials were characterized using FESEM, FTIR, XRD, and Raman. The effect of synthesizing temperature on the morphology and structure of products was investigated. With the synthesizing temperature varied from 700 to 800, 900 and 1000 °C, sizes of the iron oxide nanoparticles before a formation of CNTs increased from 14 to 72, 98, and 119 nm, respectively. The synthesis obtained CNTs with 20-50, 20-80, and 50-100 nm in diameter, and carbon spheres with 320-730 nm in diameter, corresponded to synthesizing temperature of 700, 800, 900, and 1000 °C, respectively. Moreover, FESEM image of CNTs synthesized over alpha iron in Fe/GO composite catalyst at 900 °C revealed the optimum temperature for CVD synthesis of CNTs. The crystallinity of CNTs from Raman spectra showed the high crystallinity than 700 and 800 °C. The degree of crystallinity (I_G/I_D ratio) of products synthesized at 700, 800, and 900 °C increased from 0.76, 1.45, and 1.77, respectively.

In addition, the phase transformation of iron occurred completely within synthesizing temperature 1000 °C. The iron rich gamma phase in Fe/GO treated at 1000 °C was used to synthesize CNTs at 900 °C. The carbon-encapsulated iron nanoparticles was occurred over gamma iron after CVD of n-Hexane. Therefore, the formation of CNTs was required the alpha phase of iron.

Department: Chemical Engineering
Field of Study: Chemical Engineering
Academic Year: 2016

Student's Signature

Advisor's Signature

Co-Advisor's Signature

Co-Advisor's Signature

ACKNOWLEDGEMENTS

First of all, I would like to acknowledge the PTT Research and Technology Institute (PTT RTI) for partial financial support and experience as a research assistant in this interesting field.

I am very thankful to my thesis advisor, Assoc. Prof. Dr. Tawatchai Charinpanitkul, Department of Chemical Engineering, Faculty of Engineering, Chulalongkorn University, for introducing me in the interesting journey, included in analyst and research assistant that made my valuable experience. I am also grateful to my co-advisor, Dr. Weerawut Chaiwat, and Dr. Sira Srinives for their useful guidance, suggestion.

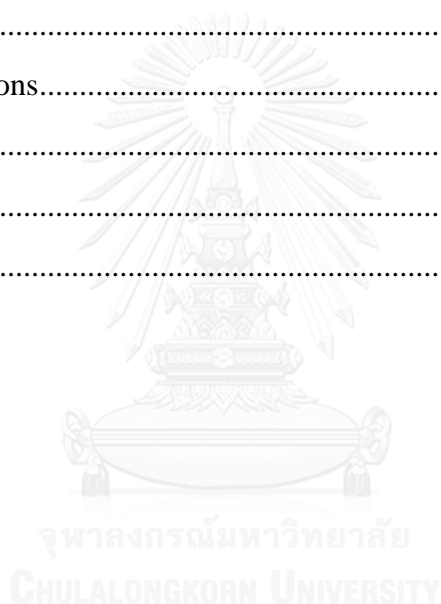
Furthermore, I would like to thank the Center of Excellence in Particle Technology (CEPT)'s members, Tawatchai's research group members, and Ms. Pusanisa Patharachotesawate for accompanying, cheering and helping me during the interval of my study.

Last but not least, I would like to express my greatest thanks to my family for their encouragement and support.

CONTENTS

	Page
THAI ABSTRACT	iv
ENGLISH ABSTRACT.....	v
ACKNOWLEDGEMENTS	vi
CONTENTS.....	vii
CHAPTER I INTRODUCTION.....	1
1.1 Motivation.....	2
1.2 Objectives	3
1.3 Scope of research	3
CHAPTER II THEORY AND LITERATURE REVIEW.....	5
2.1 Carbon nanostructures	5
2.1.1 Graphene	6
2.1.2 Carbon nanotubes	7
2.2 Preparation of Fe/GO composite	8
2.2.1 Preparation of graphene oxide using chemical exfoliation	8
2.2.2 Preparation of iron oxide nanoparticles.....	9
2.3 CVD synthesis of carbon nanotubes.....	13
CHAPTER III EXPERIMENTAL.....	16
3.1 Materials	17
3.2 CVD Reactor	17
3.3 Experimental procedures	19
3.3.1 Preparation of graphene oxide.....	19
3.3.2 Preparation of Fe/GO composite	22
3.3.3 Thermal treatment of the Fe/GO composite.....	23
3.3.4 Synthesis of CNTs on Fe/GO	24
3.4 Characterizations	25
CHAPTER IV RESULTS AND DISCUSSION.....	30
4.1 Characterization of Fe/GO composite	30
4.1.1 Functional group analysis of GO and Fe/GO composite	30

	Page
4.1.2 Elemental and thermal stability analysis of GO.....	31
4.1.3 Morphology analysis of the Fe/GO composite.....	34
4.1.4 Crystalline analysis of Fe/GO composite.....	36
4.2 Thermal treatment of Fe/GO composite	37
4.2.1 Morphology analysis of the thermally-treated Fe/GO composites	37
4.2.2 Crystallography of the thermally-treated Fe/GO composites.....	42
4.3 Synthesis of CNTs using CVD of n-Hexane on Fe/GO composite.....	43
CHAPTER V CONCLUSIONS AND RECOMMENDATIONS	53
5.1 Conclusions.....	53
5.2 Recommendations.....	54
REFERENCES	55
APPENDIX.....	59
VITA.....	68



LIST OF TABLES

	Page
Table 2.1 Methods for chemical exfoliation of graphite into graphene oxide	9
Table 2.2 Effect of iron precursors on shape and size of iron oxides	11
Table 3.1 List of chemicals	17
Table 4.1 Elemental composition of the GO	32
Table 4.2 Characteristics of carbon structure synthesized at 700-1000 °C	44
Table 4.3 BET analysis of GO and CNT/G synthesized at 700-1000°C	50
Table A1 Iron oxide particle size of as-prepared Fe/GO composite and Fe/GO composites treated at temperature of 700-1000 °C	60
Table A2 Statistical analysis of iron oxide particle size in as-prepared Fe/GO composite and Fe/GO composites treated at temperature of 700-1000 °C	62

LIST OF FIGURES

	Page
Figure 1.1 Process flow diagram of this research	4
Figure 2.1 Allotropic form of carbon: graphene and graphite	6
Figure 2.2 Structure of graphene oxide and graphene	7
Figure 2.3 Different types and various configurations of CNTs	8
Figure 2.4 SEM images of different shapes of iron oxides Nanorod (a), Nanohusk (b), distorted cubes (c), Nanocubes (d), Porous spheres (e) and Self-oriented flowers (f).....	10
Figure 2.5 TEM images of iron nanoparticles on graphene of Wang (a) and Li (b)	12
Figure 3.1 Process flow diagram of experimental procedures	16
Figure 3.2 An electric furnace with temperature control	18
Figure 3.3 Schematic diagram of tubular reactor for thermal treatment	18
Figure 3.4 Temperature profile inside the tubular reactor	19
Figure 3.5 The mixture of graphite flake, sodium nitrate and sulfuric acid	20
Figure 3.6 The mixture after adding potassium permanganate	20
Figure 3.7 The mixture after adding DI water	21
Figure 3.8 The mixture after stirring for 24 hours	21
Figure 3.9 An apparatus for filtration of graphene oxide	22
Figure 3.10 Process diagram of thermal treatment of Fe/GO composite	24
Figure 3.11 Process diagram of CVD synthesis of CNT/G hybrid materials	25
Figure 3.12 FESEM; JEOL, JSM-7610F FEG-SEM	26
Figure 3.13 EDS; Oxford Instruments, X-MaxN 20	26
Figure 3.14 FT-IR; Thermo Scientific, Nicolet 6700	27
Figure 3.15 CHN Analyzer; LECO, CHN 628 Series	28
Figure 3.16 TGA; Perkin-Elmer, TGA 8000	28
Figure 3.17 XRD; Bruker, D8 Discover	29

	Page
Figure 3.18 Raman spectrometer; Bruker, Senterra II	29
Figure 4.1 FTIR spectrum of GO (a), Fe/GO composite (b) and Iron oxide (c)	31
Figure 4.2 TGA curve of graphene oxide under a nitrogen environment	33
Figure 4.3 TGA curves of graphene oxide and Fe/GO under air and oxygen environment	34
Figure 4.4 FESEM image of as-prepared Fe/GO composite	35
Figure 4.5 PSD of as-prepared Fe/GO composite	35
Figure 4.6 EDX spectrum and elemental analysis of Fe/GO composite	36
Figure 4.7 EDX mapping of iron on Fe/GO composite	36
Figure 4.8 XRD pattern of the Fe/GO composite	37
Figure 4.9 The FESEM image of Fe/GO composite, pre-treated at 700°C	38
Figure 4.10 PSD of iron nanoparticles on the Fe/GO composite pre-treated at 700°C	38
Figure 4.11 The FESEM image of Fe/GO composite, pre-treated at 800°C	39
Figure 4.12 PSD of iron nanoparticles on the Fe/GO composite pre-treated at 800°C	39
Figure 4.13 The FESEM image of Fe/GO composite, pre-treated at 900°C	40
Figure 4.14 PSD of iron nanoparticles on the Fe/GO composite pre-treated at 900°C	40
Figure 4.15 The FESEM image of Fe/GO composite pre-treated at 1000°C	41
Figure 4.16 PSD of iron nanoparticles on the Fe/GO composite pre-treated at 1000°C	41
Figure 4.17 XRD patterns of Fe/GO composites pre-treated at 700-1000 °C	43
Figure 4.18 FESEM images of product synthesized at 700°C	45
Figure 4.19 FESEM images of product synthesized at 800°C	46
Figure 4.20 FESEM images of product synthesized at 900°C	47
Figure 4.21 PSD of CNTs synthesized at 900°C	47

	Page
Figure 4.22 FESEM images of product synthesized at 1000°C	48
Figure 4.23 Raman spectra of GO and products synthesized at 700-1000 °C	49
Figure 4.24 Relationship between SSA and total pore volume of GO and CNT/G synthesized at 700-1000 °C	51
Figure 4.25 FESEM images of product synthesized at 900°C on Fe/GO composite pre-treated at 1000°C	52
Figure B1 FESEM image of product synthesized at 700°C with magnification of 20,000X	63
Figure B2 FESEM image of product synthesized at 700°C with magnification of 100,000X	63
Figure B3 FESEM image of product synthesized at 800°C with magnification of 20,000X	64
Figure B4 FESEM image of product synthesized at 800°C with magnification of 100,000X	64
Figure B5 FESEM image of product synthesized at 900°C with magnification of 20,000X	65
Figure B6 FESEM image of product synthesized at 900°C with magnification of 100,000X	65
Figure B7 FESEM image of product synthesized at 1000°C with magnification of 5,000X	66
Figure B8 FESEM image of product synthesized at 1000°C with magnification of 50,000X	66
Figure B9 FESEM image of product synthesized at 900°C on Fe/GO composite pre-treated at 1000°C with magnification of 20,000X	67
Figure B10 FESEM image of product synthesized at 900°C on Fe/GO composite pre-treated at 1000°C with magnification of 100,000X	67

CHAPTER I

INTRODUCTION

Carbon nanostructures have long been studied and applied in various fields of application. In particular, carbon nanotubes (CNTs) and graphene are two popular carbon nanostructures that have attracted a great deal of attention, as resulted from their outstanding chemical, mechanical and electrical characteristics.

For synthesis of high quality and quantity, chemical vapor deposition (CVD) technique has been introduced in 1996 [1] and now this method is widely used for large scale production of CNTs.

High quality of CNTs have been observed when a transition metal (iron, cobalt or nickel) is used as the catalyst. Many studies have reported effect of the parameter of CVD on the synthesis of CNTs, including growth rate, diameter, morphology, and crystallinity. In the degree of crystallinity, CNTs synthesized over iron catalyst is higher than that over nickel or cobalt catalyst [2]. In CVD of CNTs over iron catalyst requires synthesizing temperature of 700-1000 °C [3-5]. These results indicate that the synthesizing temperature depend on type of transition metal catalyst. A method for preventing agglomeration of nanoparticles, the catalyst supports in heterogeneous catalysis have been established for high catalytic activity. Furthermore, parameters of CVD are consisted of carbon source, catalyst support, deposition time, gas-flow rate, pressure, and reactor geometry. In general, the molecular structure of the carbon source effect on the morphology of CNTs. Linear hydrocarbons (methane, acetylene, ethylene) are thermally decomposed by catalytic CVD into atomic carbons, and produce straight hollow CNTs [6, 7]. When graphene was used as catalyst support, carbon nanotube/graphene (CNT/G) hybrid materials could be obtained within a single step by using CVD [8]. In comparison between CNT/G hybrid materials and either pristine CNTs or graphene, their properties are extremely increased. With the result, CNT/G

hybrid materials have been developed since it could be applied in renewable energy conversion devices as supercapacitors in energy storage [9, 10] and working electrode in dye-sensitized solar cells [11].

An important role in the phase transformation of iron occurs in CVD synthesis of CNTs at temperature of 700-1000 °C. When the temperature of 910 °C has been reached, the alpha-iron begins transformation into gamma-iron at temperature of 725-740 °C [12] and becomes to gamma-iron completely [13].

1.1 Motivation

Many researchers have been developed hybrid materials of carbon nanotube and graphene by various techniques, included synthesis of graphene, CNTs, chemically bonded CNT/G. With advantages of simple technique, chemical exfoliation of graphene oxide, wet impregnation of iron oxide/graphene oxide, and CVD synthesis of CNTs were used to investigate the phenomena during synthesis of CNTs using CVD of n-Hexane in topic of temperature effect on iron oxide/graphene properties and formation of CNTs. The synthesizing temperature for CVD of CNTs over iron catalyst have been reported in range of 700-1000 °C since CVD introduced as technique for large scale production of CNTs.

For investigation effect of temperature on phase transformation of iron catalyst, the thermal treatment process exhibits the representation of iron oxide/graphene oxide composite, reduced into iron, before formation of CNTs. Effect of crystalline structures of iron (alpha-iron, gamma-iron) on formation of CNTs, the synthesis of CNTs by using CVD of n-Hexane was performed over the alpha-iron and gamma-iron within iron oxide/graphene oxide composite.

1.2 Objectives

In order to study phenomena during CVD synthesis of CNTs over iron oxide/graphene oxide composite, n-Hexane as a carbon source is converted into CNTs. Iron oxide/graphene oxide composite was thermally treated for investigation of their properties in various synthesizing temperature.

- The effect of synthesizing temperature for CVD synthesis of CNTs on properties of iron oxide/graphene composite catalyst
- The effect of synthesizing temperature on formation of CNTs over iron oxide/graphene composite catalyst

1.3 Scope of research

1) Preparation of graphene oxide

Modified Hummers method [14, 15] was used to prepare graphene oxide from natural graphite flake with -10 mesh (under size of 2 mm).

2) Preparation of iron oxide/graphene oxide composite

Wet impregnation technique [16] was used to prepare 10 wt.% of iron embedded on graphene oxide, treated in 2M of HNO_3 before impregnation, by using iron(III) nitrate nonahydrate an iron catalyst precursor.

3) Synthesis of CNT/graphene hybrid material

CVD technique was used to convert n-Hexane into CNTs with the synthesizing temperatures of 700-1000 °C.

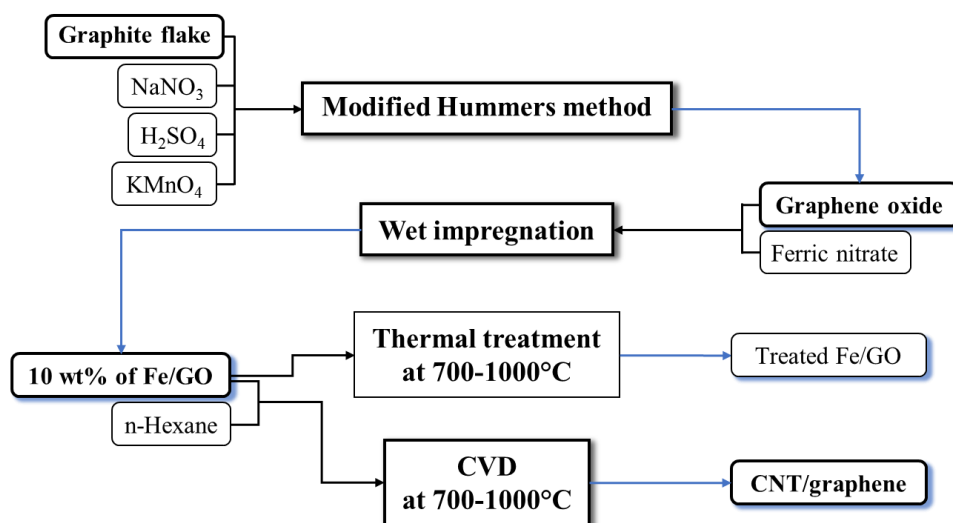


Figure 1.1 Process flow diagram of this research



CHAPTER II

THEORY AND LITERATURE REVIEW

The CVD process has long been studied and applied for synthesis of various carbon nanostructures, such as carbon nanotubes [1] and graphene [17]. Important parameters for CVD synthesis of CNTs include type of carbon source, type of catalyst and catalyst support, and operating conditions- temperature and pressure, etc. Carbon sources, used as reactant for the CNTs synthesis, can be in state of solid, liquid or gas. Popular carbon sources include methane, ethylene, and acetylene. Recently, there were reports on utilizing hydrocarbon waste as the carbon source for CNTs synthesis that involve catalytic decomposition of hydrocarbons and reformation of CNTs. Next, main catalyst for the CNTs synthesis belongs in group of transition metal, such as iron, cobalt, and nickel. To enhance surface activity of the catalyst, metal and metal oxide catalyst are made as nanoparticles, zero dimensional nanostructure with less than 100 nm in sizes. Though the metal/metal oxide nanoparticles are considered the most effective catalysts, they were suffered by interactions of surface charges on the nanoparticles that lead to particle agglomeration, and great reduction in surface activity. Catalyst support, such as porous materials and nanostructures, were used to provide solid structure for the catalyst to deposit and anchor on. The metal nanoparticles can be distributed over the support, remain separated from one another and maintain high surface area.

2.1 Carbon nanostructures

Carbon nanostructures are group of carbon-based materials with at least one dimension of less than 100 nm in size. They have become one of the most prominent platform for a wide spectrum of applications that involve surface coating, mechanical

reinforcing, adsorption materials and components in electronic devices. So far, different carbon allotropes were introduced, such as graphene [18], fullerenes [19], carbon nanohorns [20] and carbon nanotubes [21] with various outstanding characteristics, such as charge capacitance, chemical resistance, and charge transfer. Among those, the CNTs and graphene are two target of interests, creating platform for a wide range of application. Combination of the two, known as CNT-graphene hybrid, has recently been demonstrated for its unique electric capacitance and chemical adsorption ability.

2.1.1 Graphene

Graphene is a carbon allotrope, extracted from graphite that consists of layers of graphene stacked on top of one another (**Figure 2.1**).

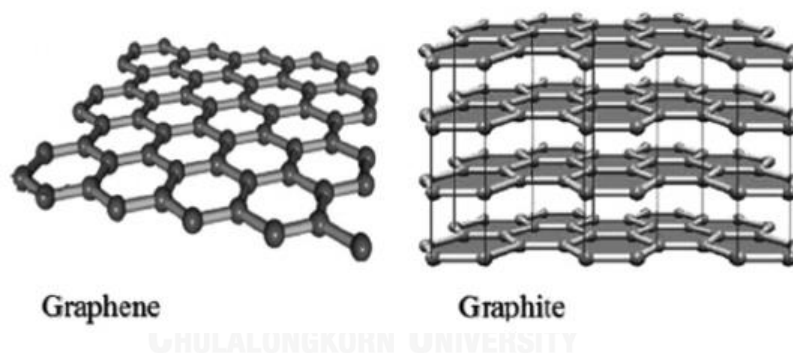


Figure 2.1 The allotropic form of carbon: graphene and graphite

After its first discover by the group of Novoselov et al. [18] from University of Manchester in 2004, graphene has attracted a great deal of attention from researcher worldwide. Interesting properties of graphene include high mobility of charge carriers ($200,000 \text{ cm}^2 \text{ V}^{-1}\text{s}^{-1}$), high thermal conductivity ($\sim 5,000 \text{ Wm}^{-1}\text{K}^{-1}$), and high specific surface area ($2,630 \text{ m}^2 \text{ g}^{-1}$) [22]. There currently are several methods for graphene synthesis, including thermal exfoliation, CVD [17], and chemical exfoliation [23]. The chemical exfoliation is one popular method that involves chemical oxidation of

graphene using strong oxidizing agent. The method yields good quality graphene in gram scale, in which graphene is oxidized and contains functional groups in its structure, known as Graphene oxide (GO). The GO structure refers to the graphene oxide sheets with oxygen-containing functional groups (**Figure 2.2**), such as carboxyl, hydroxyl and epoxy [22, 24].

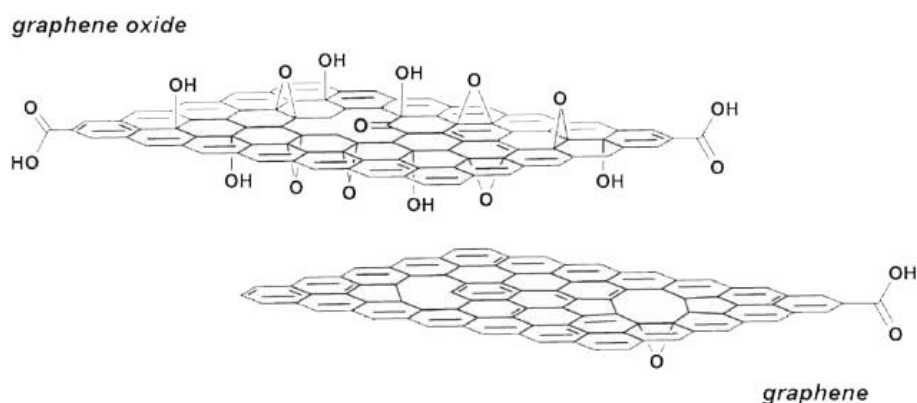


Figure 2.2 Structure of graphene oxide and graphene

2.1.2 Carbon nanotubes

Carbon nanotubes (CNTs) is another carbon allotrope with cylindrical nanostructure. It can be considered as a rolled up form of graphene layers. There are two types of CNTs - Single-Walled Carbon Nanotubes (SWCNTs) and Multi-Walled Carbon Nanotubes (MWCNTs), defined by the number of their graphitic layers. Moreover, there are three distinct ways to roll cylindrical structure, described as zigzag, armchair, and chiral (**Figure 2.3**).

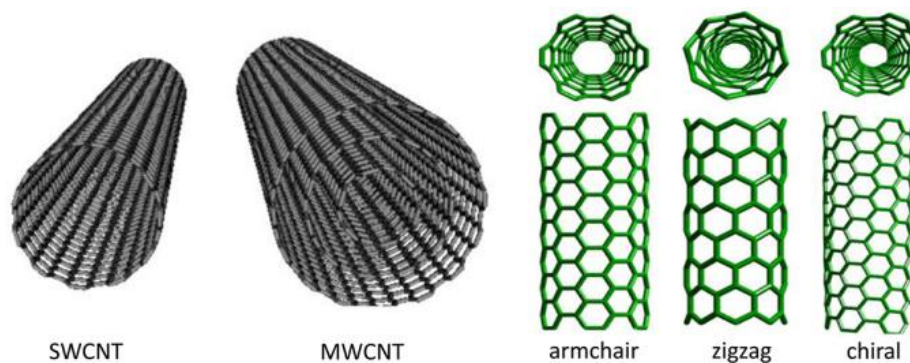


Figure 2.3 Different types and various configurations of CNTs [25]

Various techniques have been developed for a synthesis of CNTs, included arc discharge, laser ablation, and CVD. The CVD technique have been considered as the best process for commercial production of CNTs [1], due to its well-developed technology, scalable process, and good product quality. In a CVD synthesis, quantity and quality of the CNTs depend on various parameters, such as medium conditions, carbon source, catalyst, gas flow rate, reaction temperature, reaction time, pressure, and reactor geometry, etc. In this research, we focus in studying effect from thermal treatment temperature to as the CNTs growth on iron oxide/graphene composite, using n-Hexane as carbon source. The graphene was firstly synthesized following chemical exfoliation path, and further composited with the iron oxide nanoparticles via metal impregnation method. The composite was employed in an in-house CVD apparatus and used as the catalyst for the CNTs synthesis. The CNT-graphene hybrid was obtained while effects from the thermal treatment temperature were investigated.

2.2 Preparation of Fe/GO composite

2.2.1 Preparation of graphene oxide using chemical exfoliation

Chemical exfoliation of graphene was firstly introduced by Brodie (1859) [26], Staudenmeier (1898) [27], and Hummers (1958) [23]. The method was made popular

following great discovery on graphene outstanding chemical, electrical, and mechanical characters in 2004 [18]. Since then, chemical exfoliation methods have been studied, developed, and improved, providing good quality of graphene in great quantity. The methods generally involve chemical oxidation of highly crystalline graphite with strong oxidizing agent, inflicting oxygen-containing functional groups on graphite and exfoliating our graphene layers. Types of oxidizing agents, reaction time, product quality, and degree of GO oxidation can be varied, depending on the protocol of each process (**Table 2.1**). The GO is rich in functional groups that can act as electron traps, making the GO electrically insulating. Chemical reduction can be performed on the GO to partially remove functional groups from the GO structure, converting GO to reduced graphene oxide (rGO) that is semiconducting.

Table 2.1 Methods for chemical exfoliation of graphite into graphene oxide

	Brodie	Staudenmaier	Hummers	Modified Hummers	
Chemicals	KClO ₃ , HNO ₃	KClO ₃ (or NaClO ₃), HNO ₃ , H ₂ SO ₄	NaNO ₃ , KMnO ₄ , H ₂ SO ₄	K ₂ S ₂ O ₈ , P ₂ O ₅ , KMnO ₄ , H ₂ SO ₄	NaNO ₃ , KMnO ₄ , H ₂ SO ₄
Reaction time	10 hours	10 days	2 hours	8 hours	5 hours
C:O atomic ratio	2.28	1.85	2.25	1.30	1.80

2.2.2 Preparation of iron oxide nanoparticles

Iron oxide nanoparticles could be synthesized by various techniques and various iron precursors. Effects of iron precursors on shapes and sizes of iron oxide nanoparticles were studied by Sayed and Polshettiwar in 2015 [28]. Six different shapes

of iron oxides could be synthesized using the same method of synthesis just by changing the iron precursors and chemical concentrations. Each of the six types of iron precursors consisted of Iron(II) sulfate heptahydrate, iron(II) oxalate dihydrate, iron(III) chloride hexahydrate, iron(III) nitrate nonahydrate, iron(II) D-gluconate dehydrate, and pentacarbonyl iron, was mixed with cetyltrimethylammonium bromide (CTAB) (soft template) and urea (hydrolyzing agent). The mixture was stirred for a certain time prior to heat treatment with microwave assisted process. The SEM images of six different shapes of iron oxides, shown in **Figure 2.4**, exhibiting Nanorod (a), Nanohusk (b), Distorted cubes (c), Nanocubes (d), Porous spheres (e) and Self-oriented flowers (f). Details on shape and size of the iron oxide nanoparticles as correlated to type of iron precursors were presented in **Table 2.2**. Since the process used in the research relies heavily on the microwave assisted heat that create temperature profile with local heat spots, it could be difficult to obtain uniform particle formation and size distribution. Based on their XRD analysis, it was revealed the iron oxides were in crystallography of α -FeOOH, β -FeOOH, α -Fe₂O₃, γ -Fe₂O₃, and amorphous [29, 30].

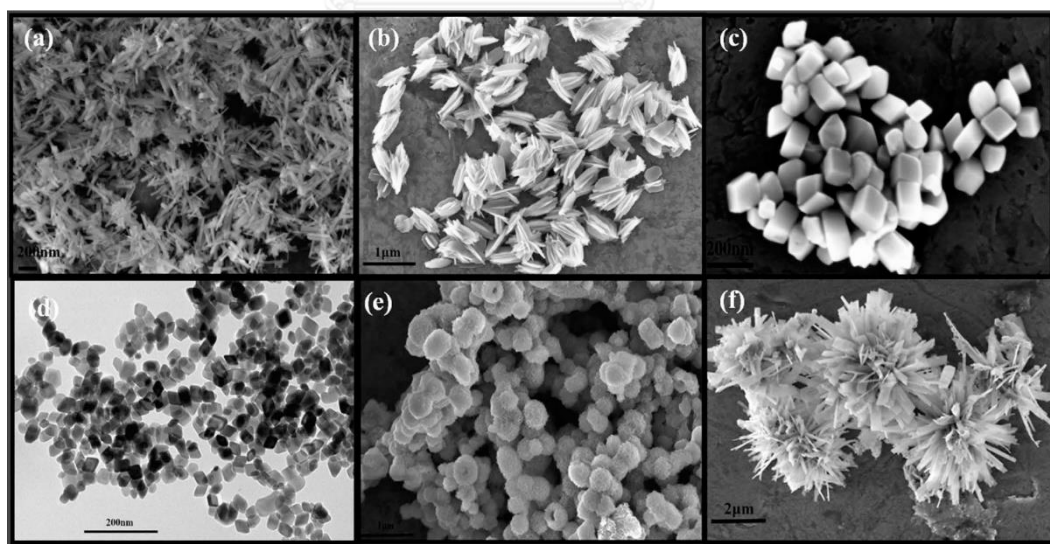


Figure 2.4 SEM images of different shapes of iron oxides Nanorod (a), Nanohusk (b), distorted cubes (c), Nanocubes (d), Porous spheres (e) and Self-oriented flowers (f)

Table 2.2 Effect of iron precursors on shape and size of iron oxides

Precursor	Shape	Phase	Size
Iron(II) sulfate heptahydrate	Nanorod	α -FeOOH	270-315 nm (length) 30-35 nm (width)
Iron(II) oxalate dihydrate	Nanohusk	β -FeOOH	803 nm (length) 369 nm (width)
Iron(III) chloride hexahydrate	Distorted cubes	α -Fe ₂ O ₃	120 nm
Iron(III) nitrate nonahydrate	Nanocubes	α -Fe ₂ O ₃ + γ -Fe ₂ O ₃	20 nm
Iron(II) D-gluconate dehydrate	Porous spheres	amorphous	150 nm
Pentacarbonyl	Self-oriented flowers	γ -Fe ₂ O ₃	250-300 nm

Composites consisting of graphene oxide and iron oxides, synthesized using iron(III) chloride as an iron precursor, also displays the iron oxide nanoparticles with a diameter of 30-60, 70-150, and 50-150 nm for using in application of composites in electrode materials [31], magnetic responsive materials [32], and reusable absorbent materials [33], respectively. As an electrode materials in supercapacitor devices (**Figure 2.4** (a)), iron oxide/graphene composite exhibits excellent electrochemical performance with large specific capacitance, good rate capability, and excellent cyclability. When pure graphene and iron oxide nanoparticles become a composite, the electrochemical performance significantly improved, compared with pure graphene and iron oxide nanoparticles. As a reusable absorbent materials (**Figure 2.4** (b)), the nanoscale zerovalent iron (NZVI) as chemical reduction technology has attracted owing to advantages of large surface area, simplicity, and low cost. Composite of nanoscale

zerovalent iron and graphene exhibits significantly higher activity, compared with pure nanoscale zerovalent iron.

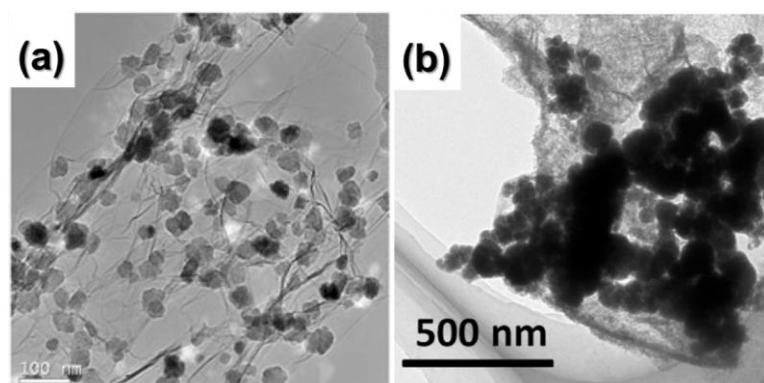


Figure 2.4 TEM images of iron nanoparticles on graphene of Wang (a) and Li (b)

As iron(III) nitrate an as iron precursor, the size of nanoparticles becomes smaller with a diameter of 1-2 and 1-5 nm using in absorbent materials by Asmaly et al. [34] and Fard et al. [16], respectively. Their composites are composed of carbon nanotubes/carbon nanofibers and iron oxide synthesized by using simple technique as a wet impregnation of iron(III)nitrate nonahydrate as an iron precursor. From theory of carbon nanotube formation, there are significant difference in surface between graphene and carbon nanotubes/carbon nanofibers as catalyst support. Graphene and carbon nanotubes are allotrope of carbon in nanostructure consisted of sp^2 - hybridized carbon arranged in a hexagonal rings of carbon. In the same configuration, carbon nanotubes were replaced by graphene oxide as catalyst support.

In addition, preparation of metal catalysts, transition and noble metals are widely used as active component in the catalysts and generally used metal salt precursors. Metal nitrates are generally introduced as a precursors over other inorganic salts due to their high solubility in water and their low contamination of as-prepared catalysts. Yuvaraj et al. [35] reported that the thermal analysis of iron nitrate under either nitrogen or vacuum conditions exhibits required temperature of 440 ± 20 and

465±20 K for decomposition of nitrate and reduction of iron oxide, respectively. the temperature of 350 °C is confirmed removal of nitrate component with the calcination temperature in preparation procedure of Asmaly et al. [34] and Fard et al. [16].

2.3 CVD synthesis of carbon nanotubes

Among several techniques for synthesis of CNTs, chemical vapor deposition (CVD) is most popular and widely used due to low cost, simple set-up, and scalable. For more information of CVD synthesis, Shah and Tali [7] and Kumar and Ando [6] reviewed on parameters of CVD synthesis, including carbon sources, catalysts and catalyst supports. The utilization of waste hydrocarbon could be extended by using in CVD synthesis of CNTs as a carbon precursor. Solid, liquid and gas hydrocarbon wastes, including polypropylene [36] and heavy oil [37], was successfully synthesized CNTs with a diameter 20 and 1 nm, respectively. Besides, solid hydrocarbon (naphthalene) and iron catalyst (ferrocene) were employed for produce CNPs using CVD at atmospheric pressure by Puengjinda et al. [38] and Charinpanitkul [3].

As mentioned above, key parameters for CVD synthesis of CNTs, including carbon source, catalyst, catalyst support, and reaction temperature were studied sufficiently to proceed this research as follows:

1) The structure of the carbon source extremely effect to the morphology of as-synthesized CNTs due to decomposition efficiency of carbon source into atomic carbons. In addition, linear hydrocarbons such as methane, ethylene, and acetylene produce straight hollow CNTs, but cyclic hydrocarbons such as benzene, xylene, and cyclohexene produce curved CNTs.

2) Transition metals, including Iron (Fe), Cobalt (Co), and Nickel (Ni) are most effective catalysts for synthesis of CNTs due to high solubility of carbon in these metals at high temperature and high diffusion rate of carbon in these metals. Furthermore, the size of nanoparticles affects to the number of layers and diameter of carbon nanotubes,

including SWCNTs and MWCNTs, synthesized by transition metal nanoparticles with a few and 10 nm, respectively.

3) The various types of supporter such as alumina, calcium carbonate, calcium oxide, graphite, magnesia, quartz, silica, and zeolite are widely used in heterogeneous catalysis to support the active site of catalysts. Either physical or chemical interactions prevent the agglomeration of catalyst nanoparticles on supporter and maintain the size distribution of the catalyst nanoparticles during growth of CNTs [6, 7]. Furthermore, effect of various types of supporter on conversion of carbon source and capacity of carbon, lifetime of catalyst, and quality of CNTs were investigated by Chai et al. [39] using methane as carbon source for CVD synthesis of CNTs over cobalt on various catalyst supports. With reaction temperature of 550 °C, silica as supporter shown the highest capacity of carbon (silica > zeolite > alumina > ceria > titania > magnesia > calcium oxide). An increase in synthesizing temperature to 700 °C, alumina shown the highest capacity of carbon, conversion of methane, lifetime of catalyst and quality of CNTs than other supporters.

4) Based on iron catalyst for CVD synthesis of CNTs, the formation of CNTs requires the temperature window of 600-700 °C [4], 800-900 °C [3, 38], 1000 °C [5]. They reported the high quality of CNTs, synthesized at various temperature. Thus, the temperature window of 700-1000 °C were investigated in this research. When graphene had become to catalyst support for carbon nanotube formation, as-synthesized CNTs became to CNT/G hybrid materials.

In recent years, hybrid materials of CNTs and graphene have attracted much attention due to outstanding properties. With a high surface area materials, CNT/G hybrid materials are useful in electronic devices [9, 10, 40].

In comparison with synthesis procedure of them, Zhu et al. [10] used CVD technique to synthesize graphene and carbon nanotube hybrid materials, Fan et al. [9]

used modified Hummers method to prepare graphene oxide, CVD technique to prepare CNTs, and thermal reduction to bond the graphene oxide and CNTs together, and Tung et al. [40] used modified Hummers method to prepare graphene oxide, used impregnation technique to embed cobalt on graphene oxide, arc discharge technique to prepare CNTs, and chemical reduction to bond the graphene oxide and CNTs together.

For example, synthesis procedure of Zhu et al. [10] consisted of 1) The CVD synthesis of graphene on a copper substrate. 2) The PVD synthesis of iron and alumina thin films on as-synthesized graphene. 3) The CVD synthesis of on graphene supported iron thin films. With a conditions of 3 nm of alumina and 1 nm of iron thickness, the CNT/G hybrid materials were obtained with specific surface area of 2285 m²/g.

In this research, a simple technique of each step was investigated to obtain the synthesis procedure with detailed explanation in Chapter 3. Briefly, the synthesis procedure for obtaining CNT/G hybrid materials with gram-scale production as follows:

- 1) Preparation of graphene oxide by using modified Hummers method
- 2) Preparation of iron oxide embedded on as-prepared graphene oxide composite through wet impregnation technique
- 3) Synthesis of CNTs on as-prepared iron oxide/graphene oxide composite via CVD technique

CHAPTER III

EXPERIMENTAL

This chapter explains an experimental details, including chemicals, experimental apparatus, experimental procedures, and methods of characterization. The experimental part can be divided to two main sections, synthesis of graphene oxide and iron oxide/graphene oxide composite, and synthesis of CNTs on iron oxide/graphene oxide composite. Effects of thermal treatment was observed from iron oxide/graphene oxide composite samples and CNT/G hybrid samples.

Overview of the experimental procedures is presented in the flow chart (**Figure 3.1**), where the graphite flakes are chemically oxidized to graphene oxide (GO), and the GO is impregnated with iron oxide to become iron oxide/graphene composite (Fe/GO). The Fe/GO composite is used as a substrate for the CNTs/GO hybrid production via the CVD process.

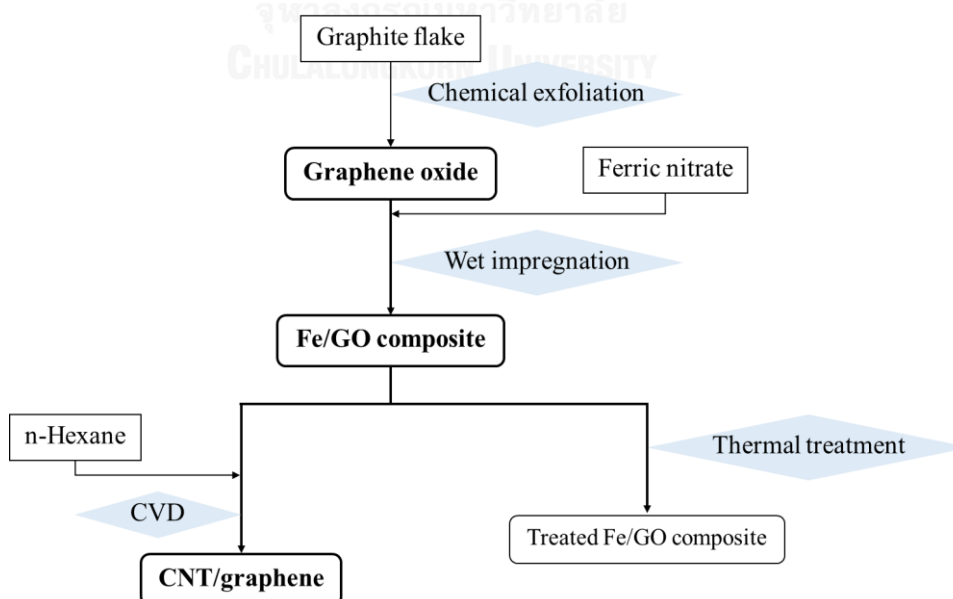


Figure 3.1 Process flow diagram of experimental procedures

3.1 Materials

All chemicals were of analytical grade and used as received with no further treatment. Lists of the chemical, used in preparation of GO, Fe/GO composite and synthesis of CNT/G can be found in **Table 3.1**.

Table 3.1 list of chemicals

Chemicals	Used for	Manufacturer
Graphite flake (~10 mesh)	Preparation of GO	Alfa Aesar
Potassium permanganate		Ajax Finechem
Sodium nitrate		Ajax Finechem
Sulfuric acid 98%		Qrec
Hydrochloric acid 37%		Qrec
Hydrogen peroxide 30%		Qrec
Iron (III) nitrate nonahydrate	Preparation of Fe/GO	Ajax Finechem
Nitrogen gas 99.999%	CVD synthesis of CNTs	LINDE
Hydrogen gas 99.99%		LINDE
n-Hexane		Carlo erba

3.2 CVD Reactor

A CVD apparatus consists of a tubular reactor- quartz tube with 4 cm inner diameter and 100 cm length, and an electric furnace (**Figure 3.2**). The electric furnace and control reaction temperature in a range of 350 to 1000 °C. The supplied gases,

nitrogen and hydrogen gases, were introduced to the CVD apparatus via two separated mass flow controllers (MFCs), and were captured in a water trap through the effluent line (Figure 3.3).



Figure 3.2 An electric furnace with temperature control

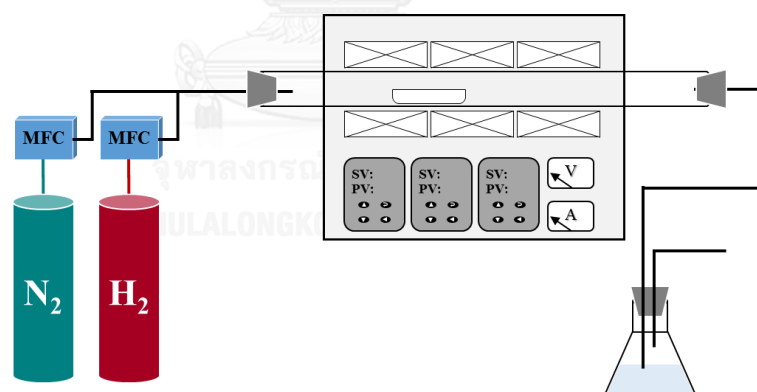


Figure 3.3 Schematic diagram of tubular reactor for thermal treatment

Temperature profile inside the tubular reactor was monitored using K-type thermocouple (Figure 3.4). All of our synthesis experiments were conducted by positioning the Fe/GO composite within the 30 to 50 cm region, where the temperature profile was relatively constant.

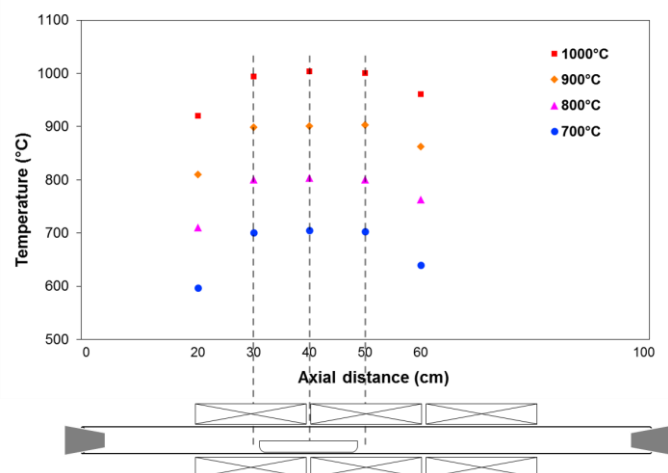


Figure 3.4 Temperature profile inside the tubular reactor

3.3 Experimental procedures

3.3.1 Preparation of graphene oxide

The GO powder was synthesized in house following a Modified Hummers method is a chemical process that can be used to produce graphene oxide using graphite flake and necessary chemical including potassium permanganate, sodium nitrate, and sulfuric acid. Next, the solution of residual permanganate was separated from graphene oxide by leaching. Then the graphene oxide with oxygen-containing functional groups was obtained in brown-black powder. The preparation of graphene oxide was divided to 8 steps as follows:

1) Graphite flakes of 5 grams was mixed with sodium nitrate of 2.5 grams in a concentrated sulfuric acid (98%) solution of 120 mL.

2) The mixture was stirred in an ice bath at 0 °C (**Figure 3.5**) for 2 hours while 15 grams of potassium permanganate was slowly added in. The mixture temperature was maintained well below 5 °C at all time during the operation (**Figure 3.6**).



Figure 3.5 The mixture of graphite flake, sodium nitrate and sulfuric acid

3) Temperature of the mixture was raised to 30 °C, and held there for 12 hours, allowing the crystalline graphite to be oxidized, becoming GO.

4) Up to this point, the mixture became viscous, as resulted from exothermic oxidation reaction that led to water evaporation. The DI water of 150 mL was poured into lower viscosity of the mixture, causing mixture temperature to rapidly raise to 98 °C. The yellow-brown color GO was observed, suspended in the mixture (**Figure 3.7**).



Figure 3.6 The mixture after adding potassium permanganate



Figure 3.7 The mixture after adding DI water

5) The suspension was stirred at 98 °C for 24 hours to complete oxidation reaction. The mixture color converted to dark brown, as resulted from water evaporation (**Figure 3.8**).



Figure 3.8 The mixture after stirring for 24 hours

6) A solution of 30% H_2O_2 of 50 mL was added to the mixture to convert residual manganese to soluble manganese (II) sulfate.

7) The GO powder was obtained using vacuum filtration apparatus, rinsed by 5% hydrochloric acid for three times, followed by DI water (**Figure 3.9**).

8) The obtained powder of GO was dried for 24 hours in an oven at 60 °C to remove the remaining moisture.



Figure 3.9 An apparatus for filtration of graphene oxide

3.3.2 Preparation of Fe/GO composite

The GO contains functional groups, such as carboxyl, hydroxyl, and carbonyl on its structure. The functional groups can dissociate in aqueous solution, giving negative polar that accumulate cations nearby. By suspending GO powder in a solution of iron salt, functional groups on GO can attract Fe^{2+} and Fe^{3+} radicals, creating preferential spots for metal deposition or metal impregnation [31, 32, 41].

For a preparation of Fe/GO, percent weight of GO and iron radicals was controlled. For example, to synthesize 10 wt% of Fe/GO composite, iron(III) nitrate nonahydrate of 0.8038 grams, which yielded iron radical of 0.1111 grams was added in a suspension of 1 gram GO in DI water. The Fe/GO was synthesized here following 4 major steps:

1) The GO powder was suspended in 200 mL of 2M HNO_3 , activated by ultrasonication for 1 hour.

2) A solution of iron radicals, containing 0.8038 grams of iron (III) nitrate in 50 mL DI water, was slowly poured to the GO suspension, and was sonicated for 3 hours.

3) The suspension was evaporated at 100 °C on the hot plate stirrer to remove excess water.

5) The Fe/GO was obtained after the sample was calcinated in a tubular reactor under nitrogen environment at 350 °C for 4 hours. Then, the Fe/GO was obtained and kept in a desiccator for future uses.

3.3.3 Thermal treatment of the Fe/GO composite

Thermal treatment can affect size and crystallography of iron oxide nanoparticles. It is worth exploring how the thermal treatment affect Fe/GO composite. The operations were performed in the CVD tubular reactor with no introduction of n-Hexane. **Figure 3.10** shows process diagram of thermal treatment of Fe/GO composite.

1) The Fe/GO composite was positioned in an alumina boat at the center of the tubular reactor while the tubular furnace conditioned it at a set point temperature.

2) Nitrogen and hydrogen gases were mixed at 1:1 volumetric ratio with a total flow rate of 100 mL/min to create a reducing atmosphere for the Fe/GO. Temperature inside the tubular furnace was raised at a heating rate of 30 °C/min to a set point temperature of 700, 800, 900 or 1000 °C. Amount of time spent on ramping up temperature to the set point was 23, 26, 29, or 33 minutes, respectively.

3) The Fe/GO samples were held at set point temperature for 10 minutes for the purpose of thermal treatment.

4) The Fe/GO was cooled down to room temperature under pure nitrogen atmosphere.

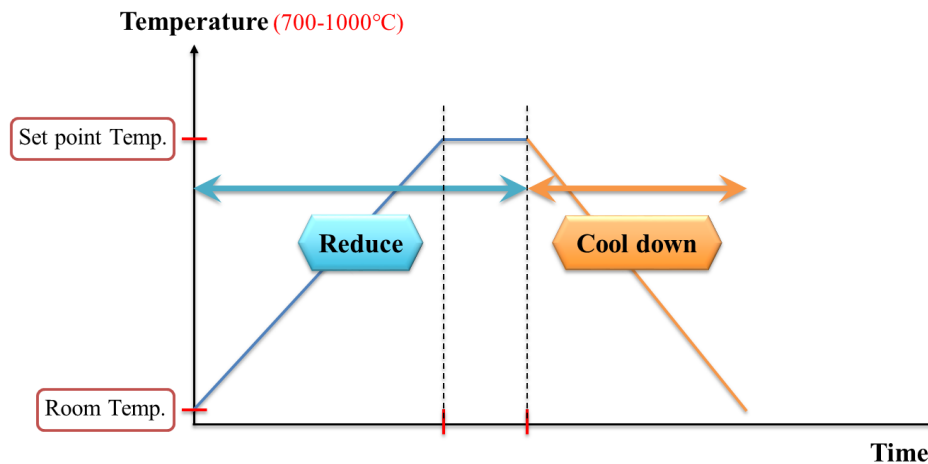


Figure 3.10 Process diagram of thermal treatment of Fe/GO composite

3.3.4 Synthesis of CNTs on Fe/GO

Synthesis of carbon nanotube on the Fe/GO was performed using the CVD technique, which is simple and scalable. The CVD synthesis of CNTs on Fe/GO consists of 6 steps, as follows:

- 1) The Fe/GO composite was positioned in an alumina boat at the center of a tubular reactor.
- 2) Nitrogen and hydrogen gases were mixed at a volumetric ratio of 1:1 and a total flow rate of 100 mL/min. The Fe/GO sample was cured in the reducing environment at set point temperature, varied from 700 to 800, 900, to 1000 °C, respectively.
- 3) The Fe/GO composite was held at the set point temperature for 10 minutes.
- 4) The nitrogen gas was fed at a total flow rate of 100 mL/min while the n-Hexane of 1.5 mL were fed in through a syringe pump at a feeding rate of 0.5 mL/min. The n-Hexane was vaporized immediately and carried through the tubular reactor to the Fe/GO composite (**Figure 3.11**).

5) The n-Hexane feed was stopped and the Fe/GO sample was purged in pure nitrogen gas for another 10 minutes at the set point temperature.

6) The Fe/GO sample was cooled down to room temperature under pure nitrogen gas.

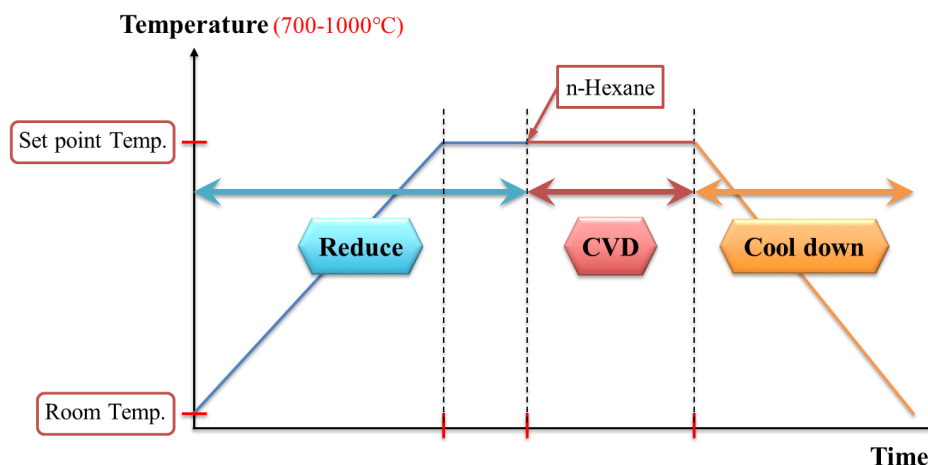


Figure 3.11 Process diagram of CVD synthesis of CNT/G hybrid materials

3.4 Characterizations

In this work, physical and crystallographic properties of the carbon materials were our main target of interest. The GO, Fe/GO composite, thermally-treated Fe/GO composites, and CNT/G hybrid material were characterized via proper analytical instruments. The field emission scanning electron microscope (FESEM), energy dispersive x-rays spectroscopy (EDX), Fourier transform infrared spectroscopy (FT-IR), carbon-hydrogen-nitrogen (CHN) elemental analyzer, thermogravimetric analyzer (TGA), X-ray powder diffraction (XRD), and Raman spectrometer were used for characterization of Fe/GO composite and CNTs/graphene hybrid.

1) FESEM and EDX

The FESEM is a high performance SEM that reveals surface geometry of a solid and conductive sample. In our case, the Fe/GO composite, thermally treated

Fe/GO composite, and CNT/G hybrid were sprinkled on an adhesive carbon tape, attached to the FESEM holder. The FESEM (JEOL, JSM-7610F FEG-SEM, USA) was operated at an accelerating voltages of 5 kV (**Figure 3.12**). The FESEM was attached to the EDX (Oxford Instruments, X-Max^N 20, England) (**Figure 3.13**), which provides elemental analysis of the sample. The qualitative and quantitative EDX analysis can be obtained.



Figure 3.12 FESEM; JEOL, JSM-7610F FEG-SEM



Figure 3.13 EDX; Oxford Instruments, X-Max^N 20

2) FTIR

The FTIR (Thermo Scientific, Nicolet 6700, USA) (**Figure 3.14**) was used to indicate infrared spectrum adsorption of certain chemical bonds from the Fe/GO samples. The infrared spectrum was scanned from 400 to 4000 cm^{-1} to provide the FTIR spectra of the sample.



Figure 3.14 FT-IR; Thermo Scientific, Nicolet 6700

3) CHN elemental analysis

The CHN Analyzer (LECO, CHN 628 Series, United States) (**Figure 3.15**) determined weight percent of carbon, hydrogen, and nitrogen in a carbon based materials. The samples would be completely combusted in pure oxygen environment and reduced to the elemental gases CO_2 , H_2O , and N_2 to determine amount of carbon, hydrogen, and nitrogen in weight percent.



Figure 3.15 CHN Analyzer; LECO, CHN 628 Series

4) TGA

The TGA (Perkin-Elmer, TGA 8000, United States) (**Figure 3.16**) was used to measure weight changes in samples as a function of temperature. The thermal characteristic and ash content of the GO and Fe/GO were characterized under pure oxygen environment.



Figure 3.16 TGA; Perkin-Elmer, TGA 8000

5) XRD

Crystallography of a sample can be characterized using the XRD (**Figure 3.17**) (Bruker, D8 Discover, Germany). Phase compositions of iron oxides

were indicated using Cu K α radiation over a 2θ range of 5-90° at room conditions. Phase indications were based on JCPDS card databases.



Figure 3.17 XRD; Bruker, D8 Discover

6) Raman spectroscopy

The Raman spectrometer (Bruker, Senterra II, Germany) (**Figure 3.18**) was used to determine degree of crystallinity of solid materials. The Raman shift spectra of the CNT/G hybrid samples presented both G peak and D peak, assigned to crystalline and non-crystalline structures, respectively.

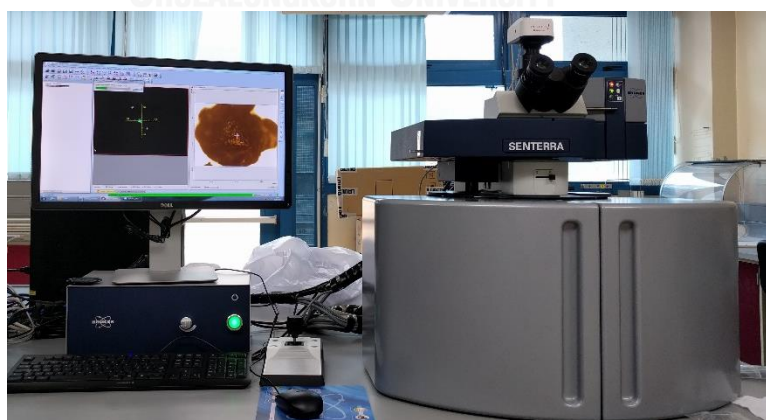


Figure 3.18 Raman spectrometer; Bruker, Senterra II

CHAPTER IV

RESULTS AND DISCUSSION

4.1 Characterization of Fe/GO composite

Chemical exfoliated graphene mostly stays in its oxidized state of GO. By oxidizing the graphite flake layers, functional groups such as carboxyl, carbonyl, hydroxyl, and epoxy are introduced to graphene structure, becoming the GO. Electrostatic charges on the functional groups create electrostatic forces that repulse GO layers from one another, make the GO suspended in aqueous solution and stayed as separated layers. Introduction of functional groups would inflict crucial changes in chemical structure and crystallography of graphene, as observed by the analytical instruments.

4.1.1 Functional group analysis of GO and Fe/GO composite

The FTIR spectra of GO, Fe/GO and iron oxide are presented in **Figure 4.1**. In case of GO (**Figure 4.1(a)**), distinct peaks at 1724, 1408, 1570, 1208 cm^{-1} can be indicated to carboxylic groups (C=O, C-O-H), aromatic bonds (C=C), epoxide groups (C-O), respectively. This is an evident that graphene from graphite flakes is successfully transformed to GO [24]. In case of Fe/GO (**Figure 4.1(b)**), two peaks at 555 and 445 cm^{-1} are assigned to stretching vibrations of Fe-O bonds [31, 32]. It was observed that absorption peaks related to oxygen-containing functional groups of the GO are reduced after compositing with the iron oxide, indicating side reduction reaction of GO during the Fe/GO synthesis. FTIR spectra of the iron oxide (**Figure 4.1(c)**) shows the characteristic peaks at 543 and 471 cm^{-1} . It can be concluded here that GO was partially reduced and iron oxide was composited with GO during the Fe/GO synthesis.

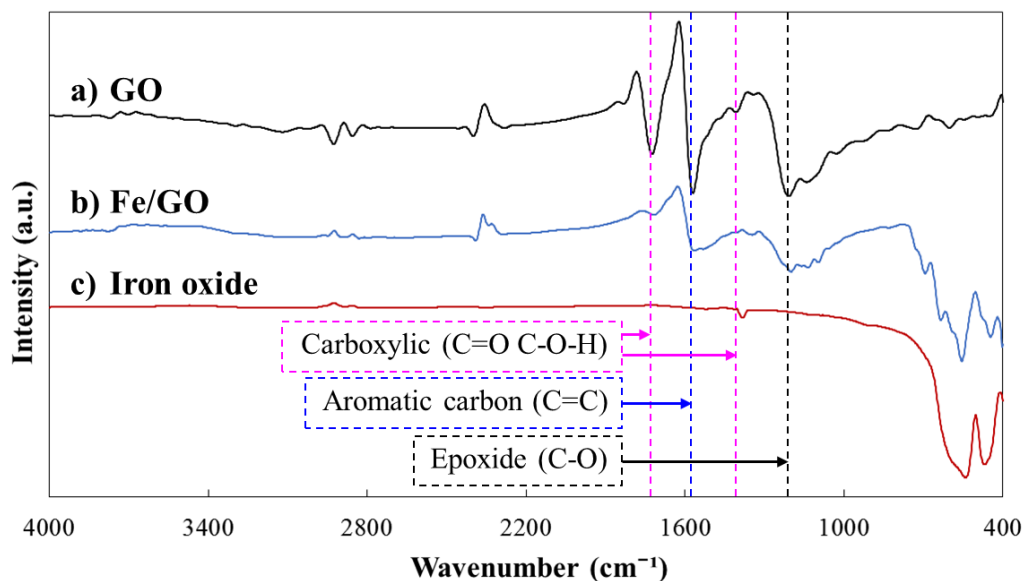


Figure 4.1 FTIR spectrum of GO (a), Fe/GO composite (b) and Iron oxide (c)

4.1.2 Elemental and thermal stability analysis of GO

Atomic ratio of carbon to oxygen (C:O) can determine amount of oxygen-containing functional groups on GO sample. We used CHN elemental analyzer to revealed weight percent and atomic percent of hydrogen, carbon, nitrogen, and oxygen in GO sample (**Table 4.1**). The C:O ratio was calculated using carbon, nitrogen, hydrogen content from CHN analyzer, oxygen content from subtracting of carbon, nitrogen, hydrogen, and ash content from the total percentage of 100. The C:O atomic ratio of 2.1:1 was obtained from 53.11 atomic percent of carbon to 25.22 atomic percent of oxygen. It's worth noting that the atomic ratio obtained here is in conformity with that from Hummers (2.25:1) [23] and modified Hummer's method of Hirata et al. (1.8:1) [42].

Table 4.1 Elemental composition of the GO

Element	Hydrogen	Carbon	Nitrogen	Oxygen
Weight (%)	2.02	59.61	0.14	37.75
Atomic (%)	21.56	53.11	0.11	25.22

The TGA curve (**Figure 4.2**) shows correlation between sample weight and temperature under a pure nitrogen environment, revealing thermal stability of the GO. Weight loss profile of the GO sample, observed in operating range of 100-1000 °C, can be divided to 3 regions. The first region started well below 200 °C and was correlated to moisture evaporation. The second region occurred between 200 to 800 °C, and was attributed to thermal decomposition of GO functional groups, e.g. carboxylic and hydroxyl groups. The third region, observed at 800 to 1000 °C, suggested thermal decomposition of epoxide groups. Beyond that, temperature of above 1000 °C caused cracking of aromatic groups [43] in GO structure. It was found that the GO carbon content from CHN elemental analysis (59.61 weight percent) showed higher weight percent than that of the GO from TGA analysis at 1000 °C (39.66 weight percent). This can be interpreted that GO structure is partially decomposed, and emitted from the TGA system within the operating temperature range of 100-1000 °C. On the other hand, the same TGA trend was observed from the Fe/GO samples, stating that GO on the Fe/GO also underwent similar path of decomposition as the GO.

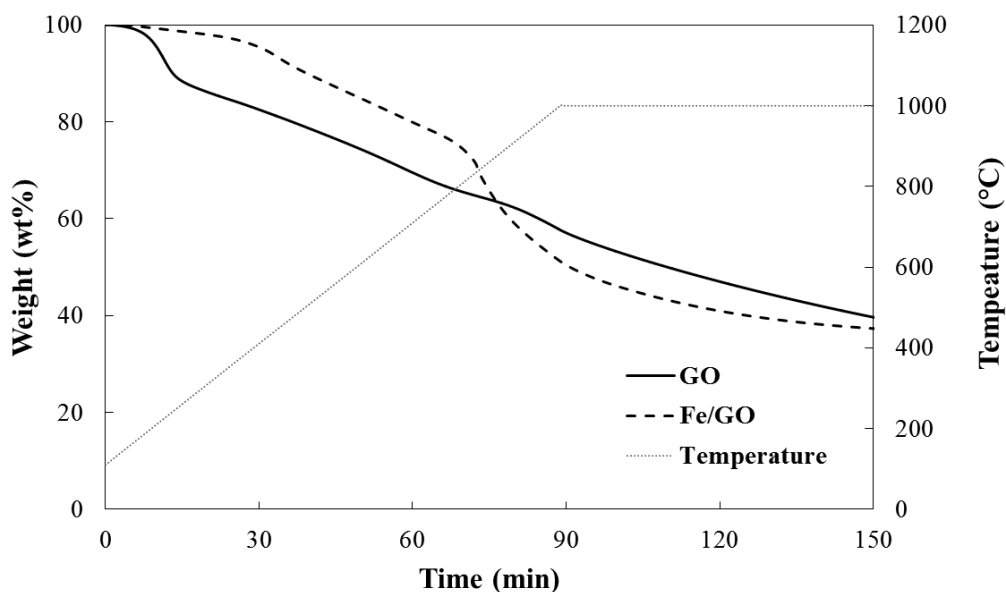


Figure 4.2 TGA curve of GO under a nitrogen environment

The TGA analysis was also performed under pure oxygen environment (**Figure 4.3**) in an operation range of 100-1000 °C. At first, 50-350 °C of operating temperature, the Fe/GO exhibits better thermal stability as compared to the GO, which can be attributed to relatively less amount of functional groups on Fe/GO as compared to GO. However, as the operating temperature exceeds 370 °C, Fe/GO shows a shoulder of significant weight loss due to presence of iron oxide that enhances combustion rate of the carbon structures [44]. In case of GO sample, the combustion shoulder appears at around 500 °C, showing higher thermal stability than that of the Fe/GO in this range of temperature (370-550 °C). It was observed that after 800 °C, GO ash weight only 0.5 % while the Fe/GO ash weight around 27.1 %. The excess weight on Fe/GO can be attributed to that of the remaining iron oxide.

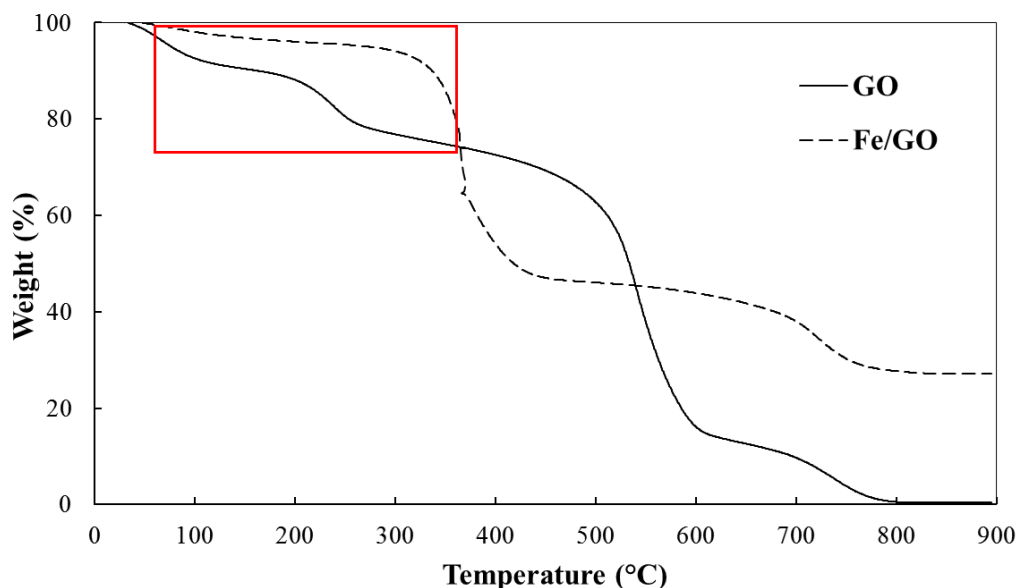


Figure 4.3 TGA curves of graphene oxide and Fe/GO under an oxygen environment

4.1.3 Morphology analysis of the Fe/GO composite

The 10% w Fe/GO composite was synthesized and positioned on the sample holder of FESEM. The FESEM images (**Figure 4.4**) depicted iron oxide nanoparticles, uniformly distributed over the GO sheets. Sizes of the nanoparticles were determined and recorded from 100 nanoparticles, observed under the FESEM. The particle size distribution (PSD) of iron oxide nanoparticles was created and revealed that the particle size of iron oxide on the GO was in the range of 3-15 nm. (**Figure 4.5**). Average particle size of iron oxide nanoparticles was 9 nm with a narrow distribution. It was noted that the iron(III) nitrate was demonstrated to yield smaller nanoparticles as compared to that of iron(III) chloride, iron(II) sulfate, iron(II) oxalate, iron(II) gluconate, and pentacarbonyliron [28].

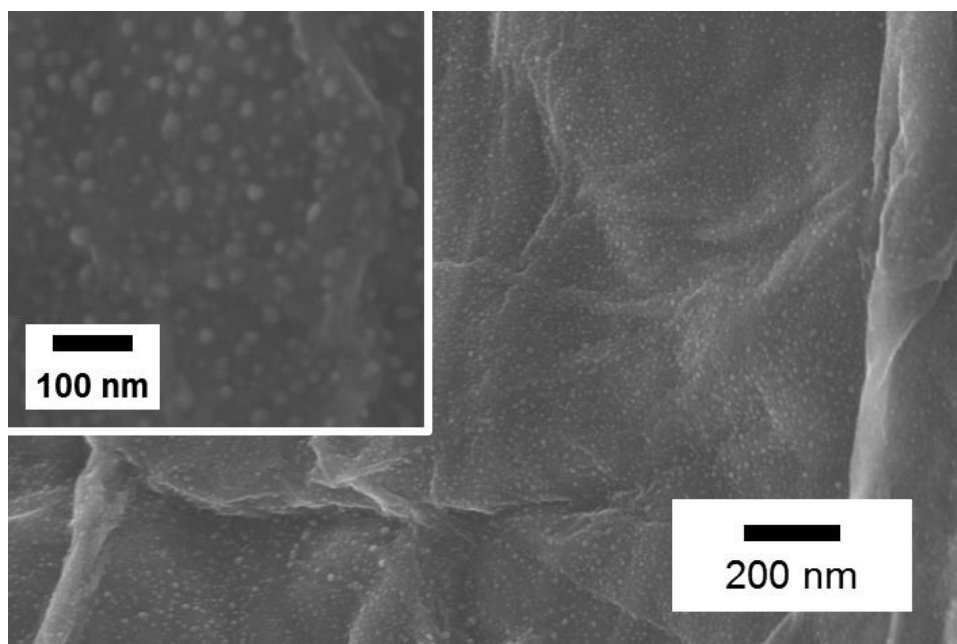


Figure 4.4 FESEM image of as-prepared Fe/GO composite

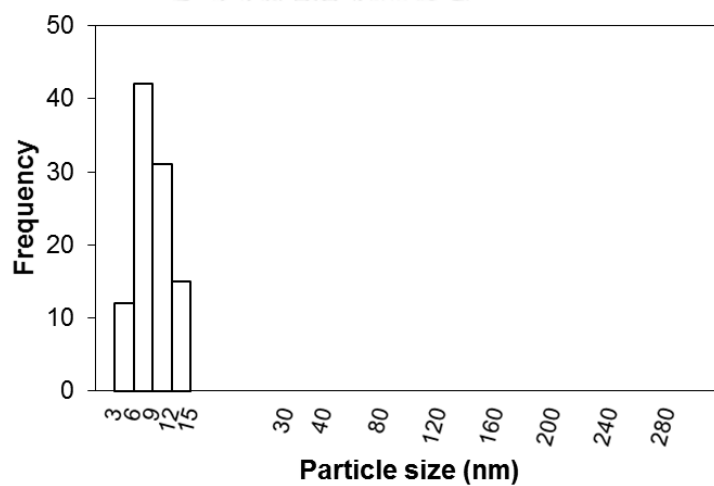


Figure 4.5 PSD of the Fe/GO composite

The EDX analysis provides element composition of the Fe/GO composite (**Figure 4.6**), showing peaks of carbon, oxygen, and iron with weight percentage of 76.1, 19.0, and 4.9, respectively. Mapping of difference elements are shown in **Figure 4.7**, revealing uniform distribution of iron oxide nanoparticles on graphene sheets.

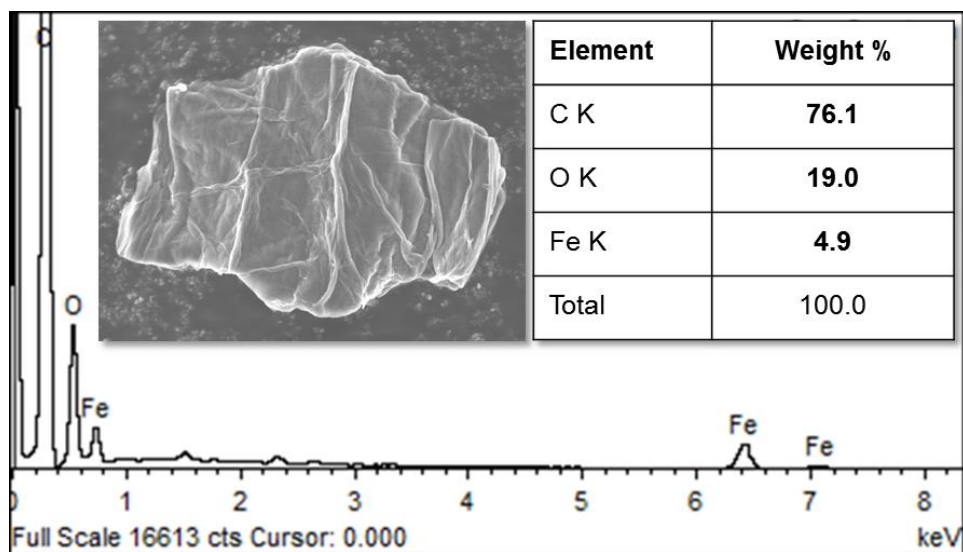


Figure 4.6 EDX spectrum and elemental analysis of Fe/GO composite

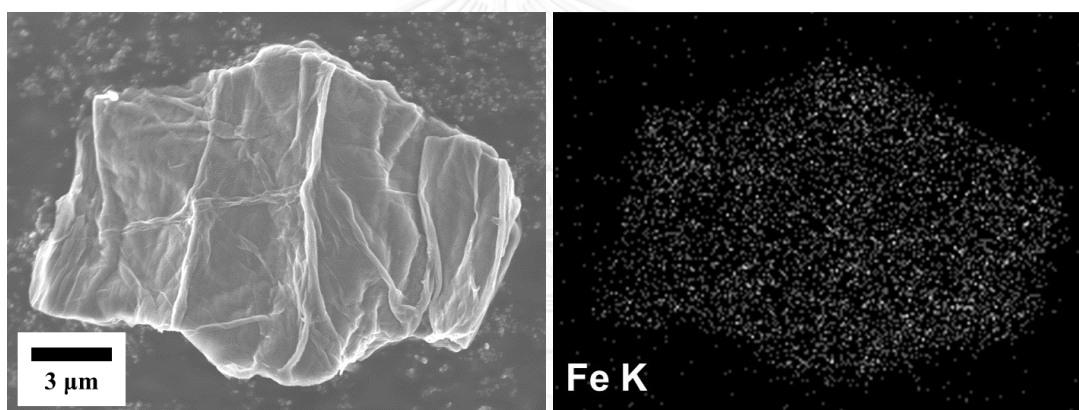


Figure 4.7 EDX mapping of iron on Fe/GO composite

4.1.4 Crystalline analysis of Fe/GO composite

The crystal structure of the Fe/GO composite was characterized using XRD (**Figure 4.8**). Peak at 26.6° can be indexed to (002) plane of graphite (JCPDS No. 26-1080) while the peaks at 29° , 25° , and 43° were matched with the γ - Fe_2O_3 [45]. It's worth noting that the XRD peaks for γ - Fe_2O_3 were poorly stated due to amorphous state of iron oxides that was previously treated at low temperature of 350°C [46].

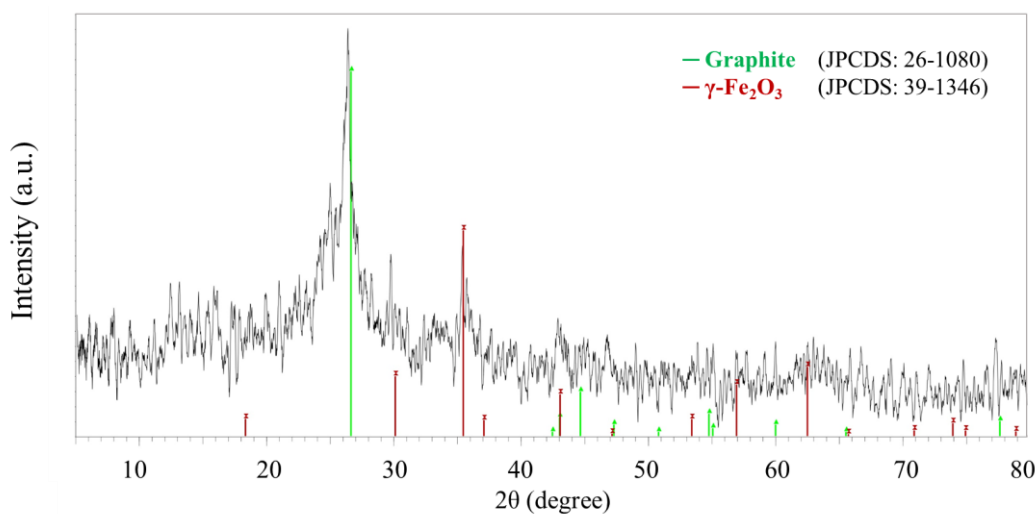


Figure 4.8 XRD pattern of the Fe/GO composite

4.2 Thermal treatment of Fe/GO composite

Effects of thermal treatment during the CNTs synthesis were investigated here on Fe/GO composite. It was reported that CVD synthesis of the CNTs depended strongly on type of catalyst and synthesis temperature [3, 4, 29, 38]. Iron oxide is one popular catalyst for synthesis of CNTs with a synthesizing temperature range of 700 to 1000 °C.

4.2.1 Morphology analysis of the thermally-treated Fe/GO composites

Morphology of the Fe/Go composites, pre-treated at temperature of 700-1000°C, were observed under the SEM, analyzing changes in geometrical properties. It was found that by pre-treating the Fe/GO composite with temperature in the range of 700 to 1000 °C, sizes and shapes of the iron oxide nanoparticles on the Fe/GO increase and change. FESEM image of the Fe/GO composite that were treated at 700°C (**Figure 4.9**) revealed spherical shape of iron oxide nanoparticles with average diameter size of

14±5 nm. Particle size distribution of the iron oxide nanoparticles is presented in **Figure 4.10** with standard deviation of 5.

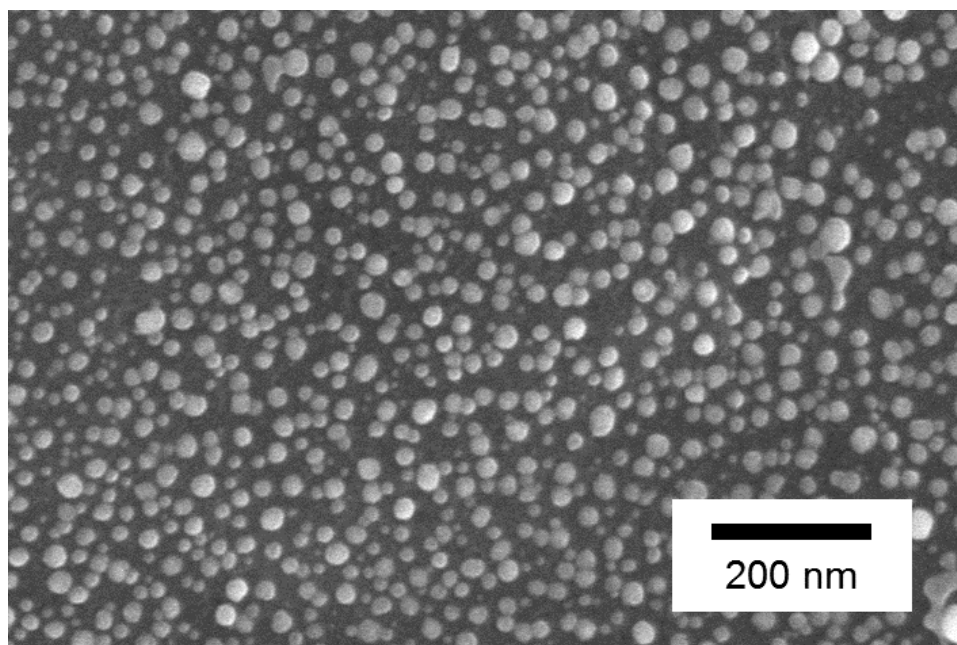


Figure 4.9 The FESEM image of Fe/GO composite pre-treated at 700°C

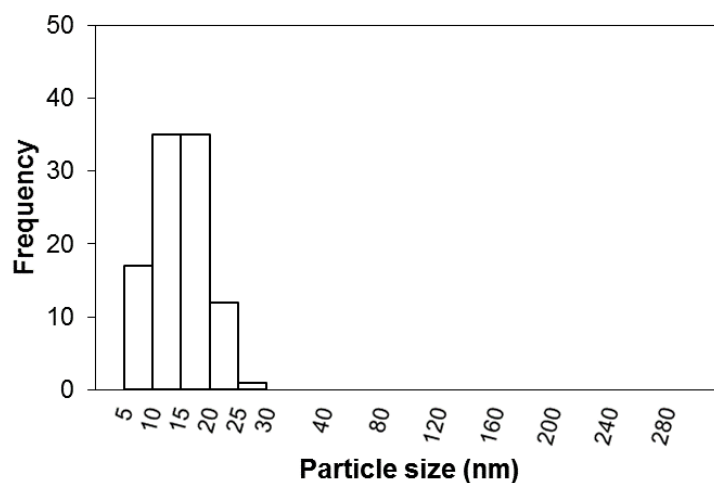


Figure 4.10 PSD of iron nanoparticles on the Fe/GO composite pre-treated at 700°C

For comparison, the Fe/GO composite, pre-treated at 800°C (**Figure 4.11**), exhibits rounded shape nanoparticles with the average particle size of 72±28 nm.

Particle size distribution is found to be broader (**Figure 4.12**), as compared to that of the Fe/GO that was pre-treated at 700 °C.

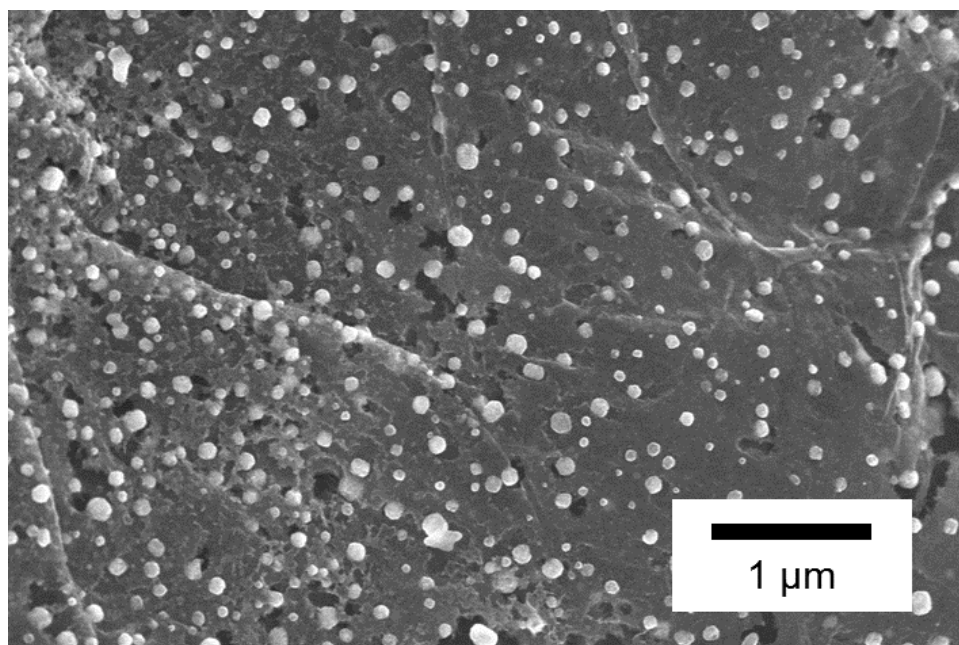


Figure 4.11 FESEM image of the Fe/GO composite pre-treated at 800°C

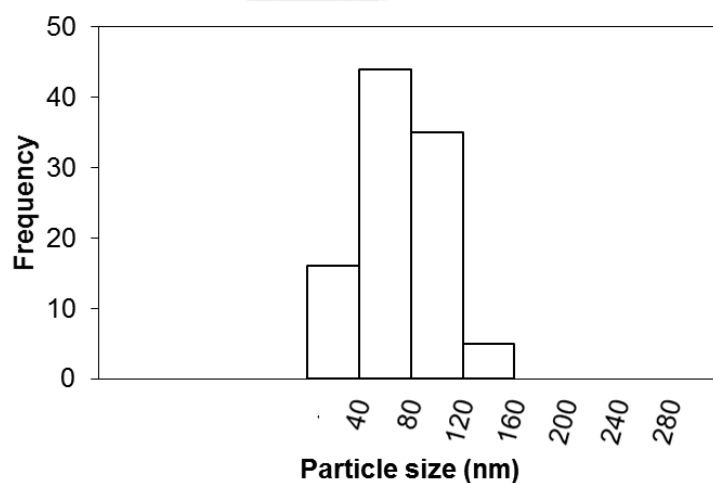


Figure 4.12 The PSD of Fe/GO composite pre-treated at 800°C

When the thermal treatment temperature increases to 900°C, shape of the iron oxide nanoparticles transformed to prismatic shape and the particle size increased to

98 ± 37 nm. (**Figure 4.13**). The particle size distribution becomes broader as shown in **Figure 4.14** with a minimum size of 41 nm and a maximum size of 228 nm. Finally, the Fe/GO composite, pre-treated at 1000°C (**Figure 4.15**), shows prismatic shape of iron oxide particles. The average particle size of iron oxide particles was 119 ± 39 nm with a broad particle size distribution (**Figure 4.16**). In addition, surface of the GO was found damaged by cracking of aromatic bonds.

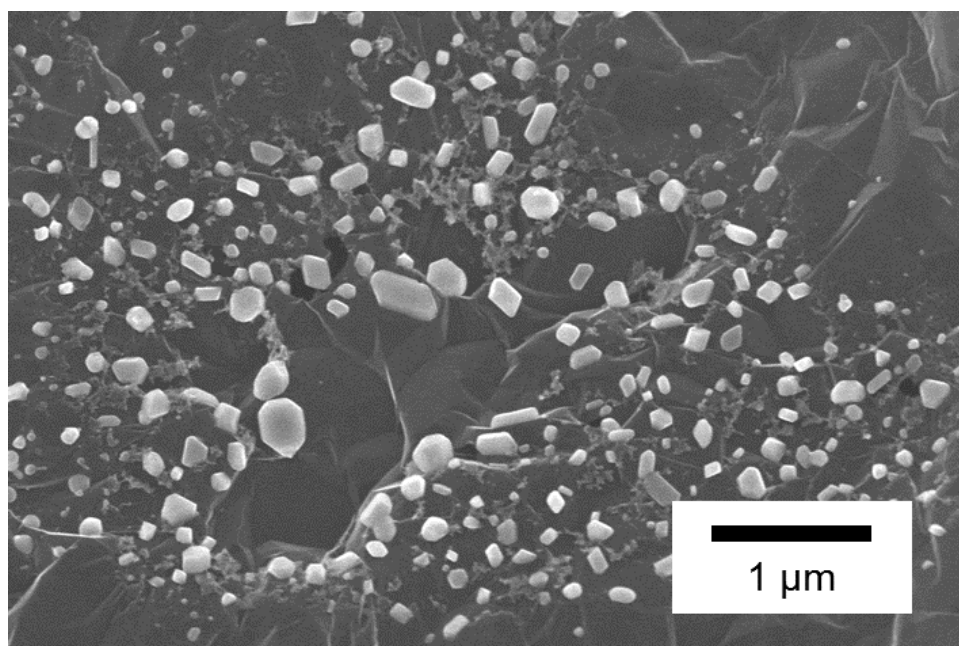


Figure 4.13 FESEM image of Fe/GO composite pre-treated at 900°C

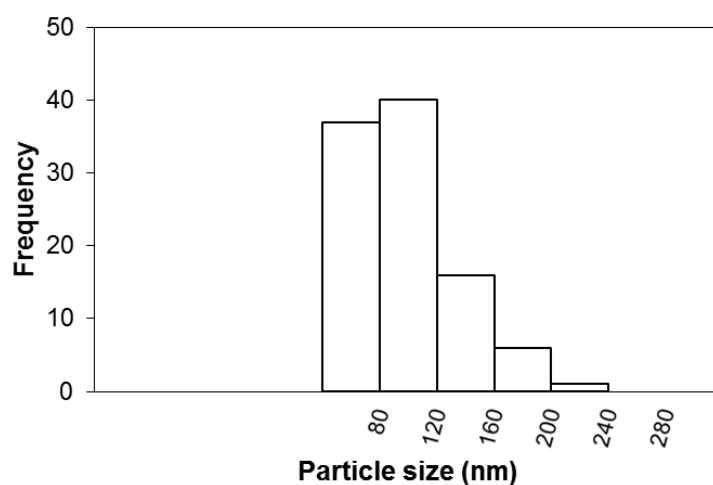


Figure 4.14 PSD of Fe/GO composite pre-treated at 900°C

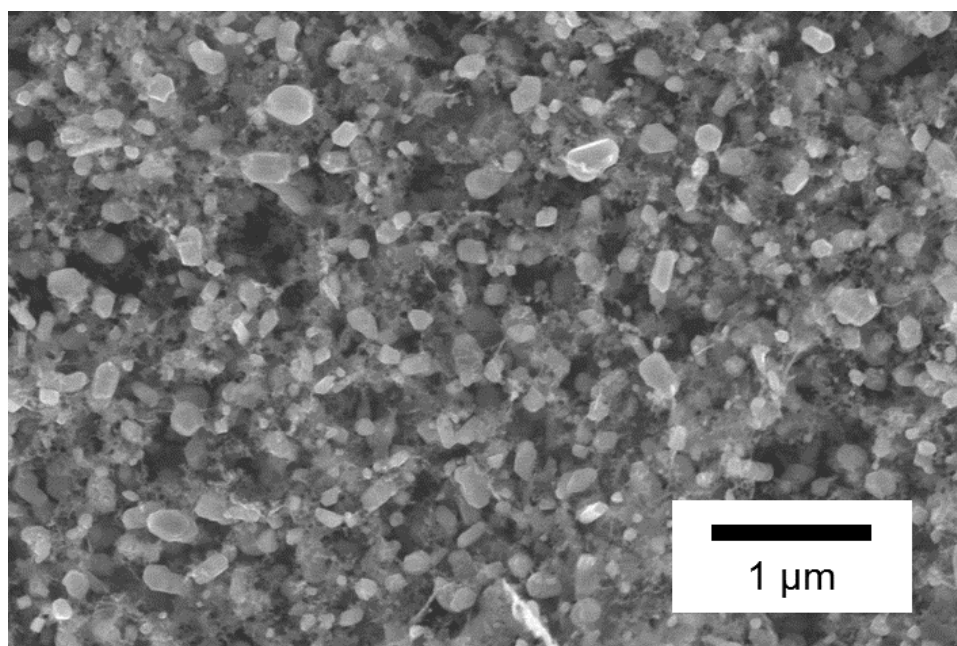


Figure 4.15 The FESEM image of Fe/GO composite pre-treated at 1000°C

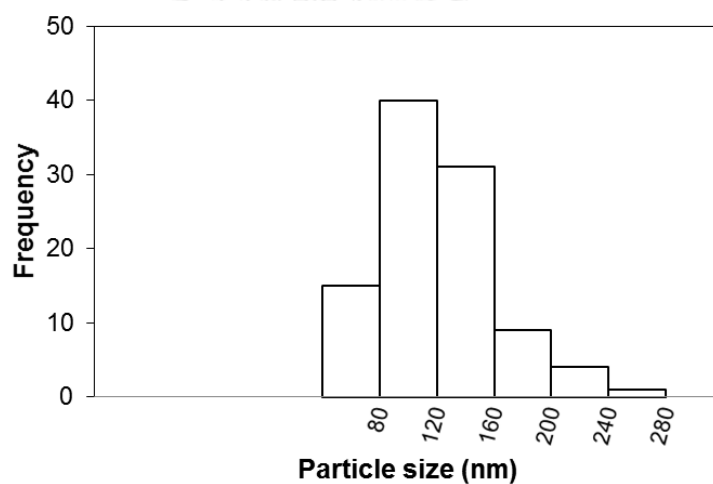


Figure 4.16 The PSD of Fe/GO composite pre-treated at 1000°C

It can be concluded that as the treatment temperature increased from 700 to 800, 900 and 1000 °C, respectively, sizes of the iron oxide particles on the Fe/GO composite increased. Besides, shapes of the iron oxide nanoparticles transformed from round shape to prismatic shape as the temperature increased from 700 to 800, 900 and 1000

°C, which can be attributed to phase transformation in iron oxide that involves changes in crystallography of the nanoparticles [45, 47].

4.2.2 Crystallography of the thermally-treated Fe/GO composites

Crystallography of the iron oxides strongly relies on its molecular forms- FeO, Fe₃O₄ (FeO·Fe₂O₃) and Fe₂O₃. Three main states of the iron oxides at room conditions are magnetite (Fe₃O₄), hematite (α -Fe₂O₃), and maghemite (γ -Fe₂O₃)[48], in which hematite and maghemite are known as alpha and gamma state of iron oxide, respectively. In the temperature window of 700 to 1000 °C, used during the CNTs synthesis, alpha-iron and gamma-iron can be transformed to one another, as supported by the XRD patterns (**Figure 4.17**). The XRD patterns of the Fe/GO composite exhibit diffraction peak at 26.4°, which can be assigned to (002) planes of hexagonal multilayered graphene [32, 41]. For the Fe/GO composite, treated at 700°C, iron oxide crystallography three diffraction peaks at 44.7°, 65.0° and 82.6°, which can be assigned to the (110), (200), and (211) planes of the hematite (α -Fe₂O₃; JCPDS No. 33-0664) [49, 50]. As the treatment temperature increase, iron oxide crystallography converts to maghemite (γ -Fe₂O₃). Diffraction peaks at 30.0°, 35.4°, 43.1°, 53.4°, 56.9°, and 62.5° matches well with (220), (311), (400), (422), (511), and (440) planes of the maghemite (γ -Fe₂O₃ ; JCPDS No. 39-1346) [51]. Diffraction peaks at 36.1°, 42.0°, and 61.0° were assigned to the FeO (JCPDS No. 06-0615) [51].

At the treatment temperature of 700 °C, the Fe/GO occurs to be pure hematite (α -Fe₂O₃). Slight transformation from hematite to maghemite was observed after the Fe/GO was thermally treated at 800 °C. It is worth noting that hematite-maghemite transformation was previously reported to start at 725-740 °C [12]. With increasing temperature from 900 to 1000, hematite transformed completely to maghemite.

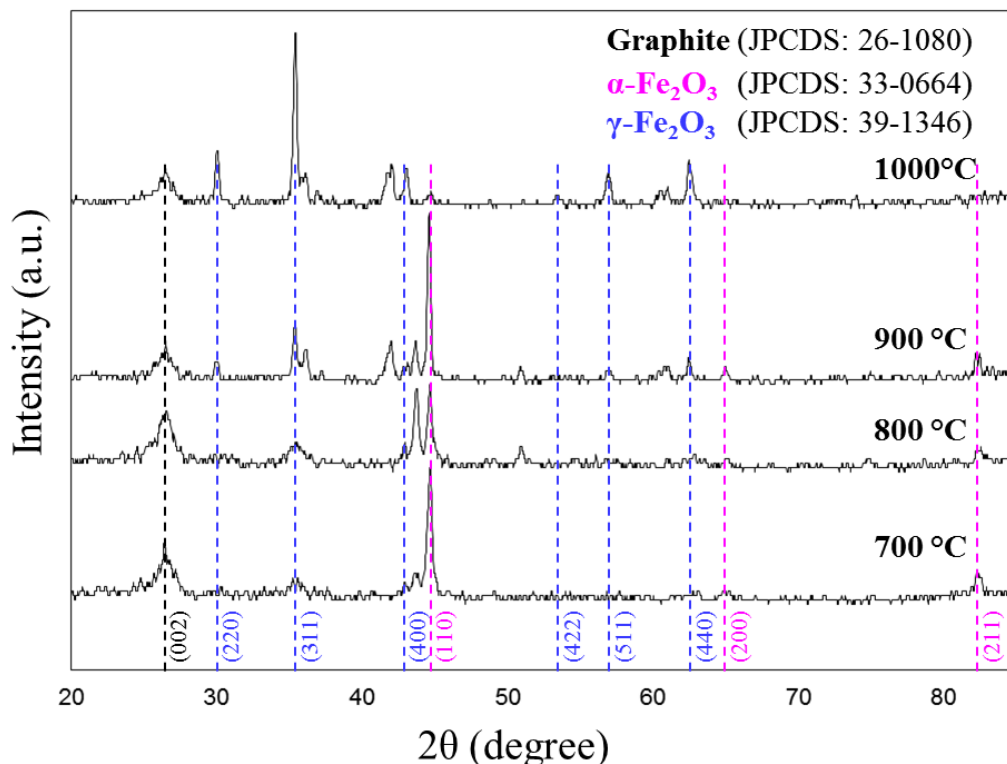


Figure 4.17 XRD patterns of Fe/GO composites pre-treated at 700-1000 °C

4.3 Synthesis of CNTs using CVD of n-Hexane on Fe/GO composite

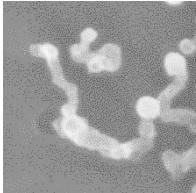
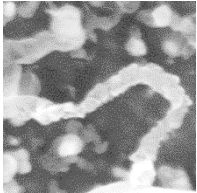
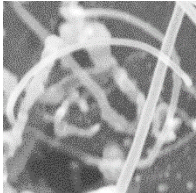
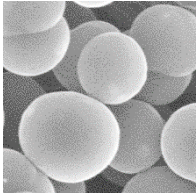
Effects from thermal treatment to the CNTs synthesis was investigated by employing the Fe/GO in the CVD apparatus and used it for the CNTs synthesis. The synthesis temperature was fixed in the range of 700 to 1000 °C, corresponded to the thermal treatment temperature.

Prior to the CNTs synthesis, sizes of the iron oxide nanoparticle were observed by the SEM to be 14 ± 5 , 72 ± 28 , 98 ± 37 , and 119 ± 39 nm, as corresponded to the treatment temperature of 700, 800, 900, and 1000 °C. The Fe/GO composites that underwent thermal treatment of 700 to 900 °C, shows mainly the alpha-iron phase (Figure 4.17). As the thermal treatment reach the temperature of 1000 °C, the alpha-iron phase was transformed to the gamma-iron phase. The Fe/GO composite that

previously treated at 1000 °C was used for a CNTs synthesis at 900 °C here to observe effects of the thermal treatment that affect crystallography of the iron oxide catalyst.

It was found here that the synthesizing temperature significantly affects shapes and sizes of the growth carbon materials. In our case, carbon nanotubes, carbon spheres, and carbon-encapsulated iron nanoparticles were observed (Table 4.2). Initially, carbon nanotubes with short length were grown on Fe/GO composite at synthesizing temperature of 700-800 °C. When the synthesizing temperature increases to 900 °C with constant other conditions, as-synthesized products were obtained with straight and hollow carbon nanotubes. With an increase in the synthesizing temperature to 1000 °C the carbon spheres were obtained with a diameter in micron-scale.

Table 4.2 Characteristics of carbon structure synthesized at 700-1000 °C

	Synthesizing temperature (°C)			
	700	800	900	1000
Structure	CNTs	CNTs	CNTs	Carbon sphere
Size (D)	20-50 nm	20-80 nm	50-100 nm	320-730 nm
(L)	100-500 nm	200 nm - 1 μm	0.5-10 μm	
Forms	Curly	Curly	Straight	Spherical
Overview images				

D = diameters of particle

L = length of particle

Under a synthesizing temperature of 700 °C, products were found that the as-synthesized products mainly consisted carbon nanotubes with entangled and coiled tubes in diameters of 20-50 nm and length of 100-500 nm as shown in **Figure 4.18**. Similarly, with higher synthesizing temperature of 800 °C, carbon nanotubes were grown like an as-synthesized products at temperature of 700 °C with larger in diameters of 20-80 nm and longer in length of 200 nm - 1 μm as shown in **Figure 4.19**. The length of carbon nanotubes depends on growth rate of formation. With other conditions constant, the synthesizing temperature affects to length of nanotubes in exponential function. From previous research of Lee et al. [29] an increase in synthesizing temperature from 750 °C to 850 °C and 950 °C, the length of CNTs was 5, 10, and 20 μm, respectively, corresponding to twofold and fourfold increase. In addition, the growth rate of Lee et al. was determined by length of CNTs per feeding time of carbon source.

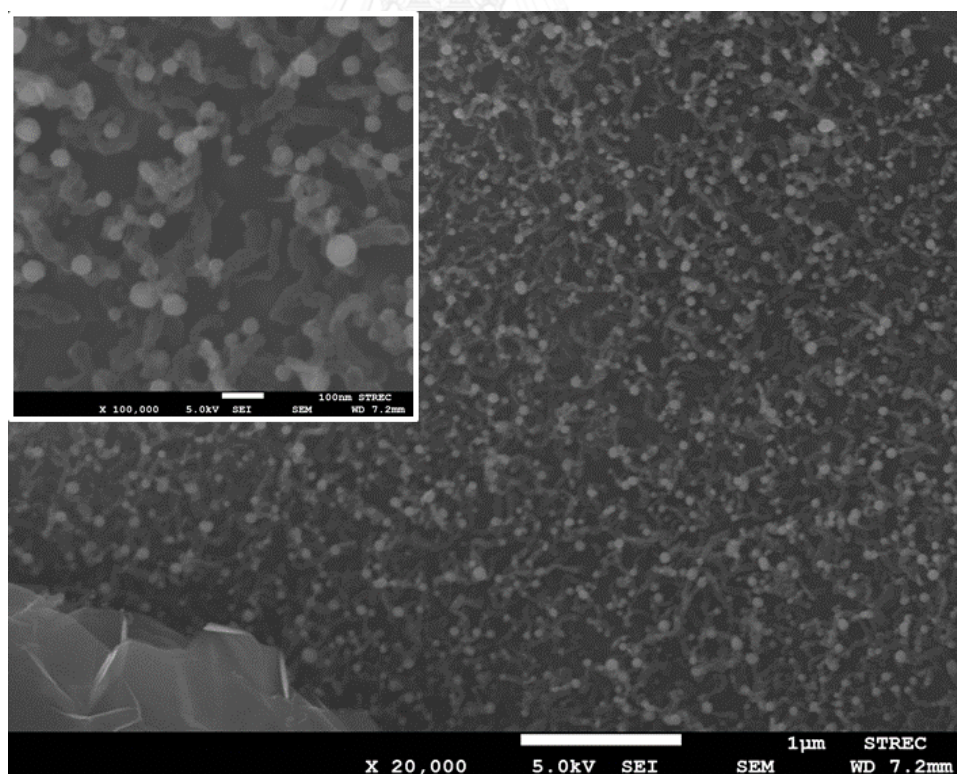


Figure 4.18 FESEM images of product synthesized at 700°C

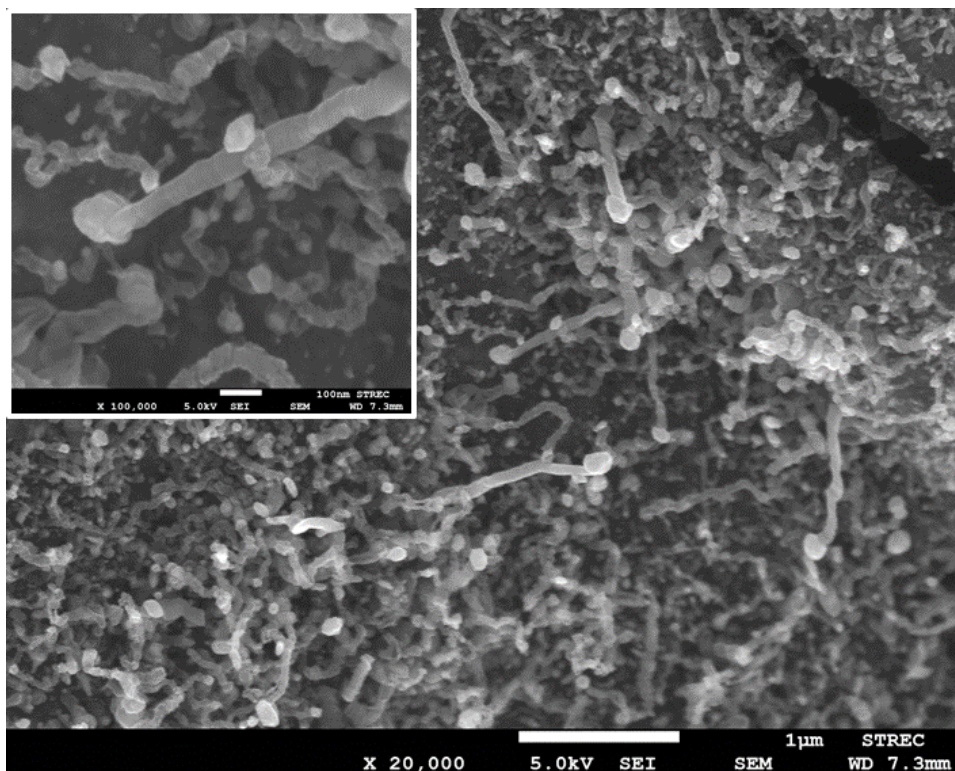


Figure 4.19 FESEM images of product synthesized at 800°C

Interestingly, an increase in synthesizing temperature to 900°C, as-synthesized products exhibited the products in the forms of straight and hollow CNTs. The characteristics of CNTs, synthesized at 900°C, exhibit 50-100 nm in outer diameters and 0.5-10 µm in length as shown in **Figure 4.20**. In these investigations, an increase in synthesizing temperature to 900°C was considered as an optimum conditions for formation of CNTs. In addition, the PSD of CNTs, synthesized at 900°C, was shown in **Figure 4.21**.

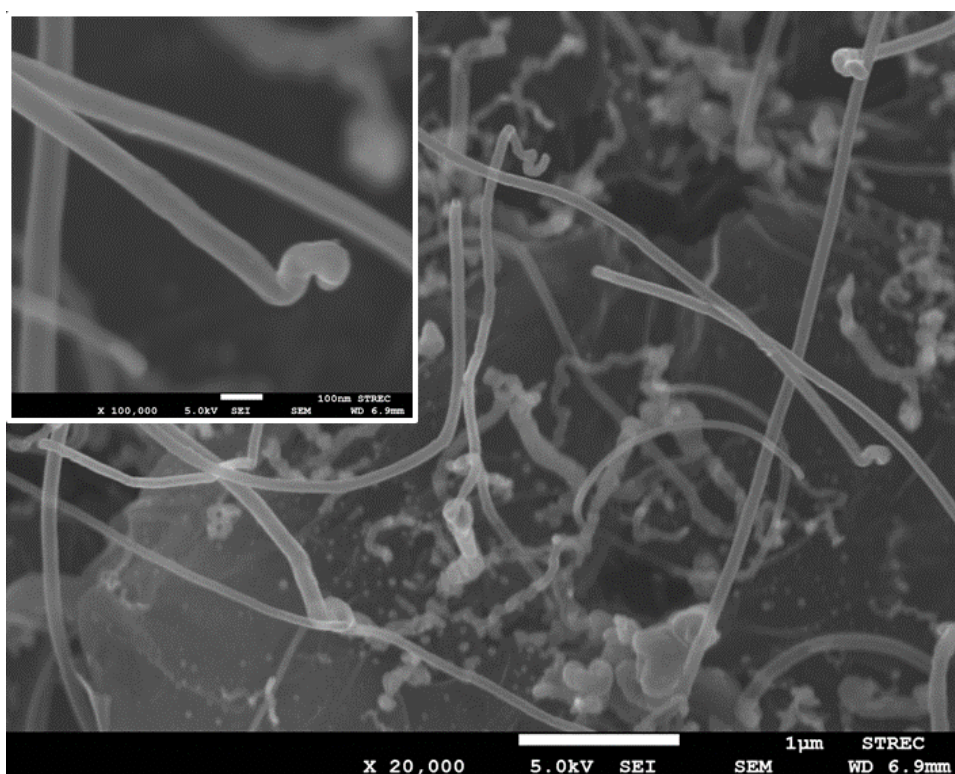


Figure 4.20 FESEM images of product synthesized at 900°C

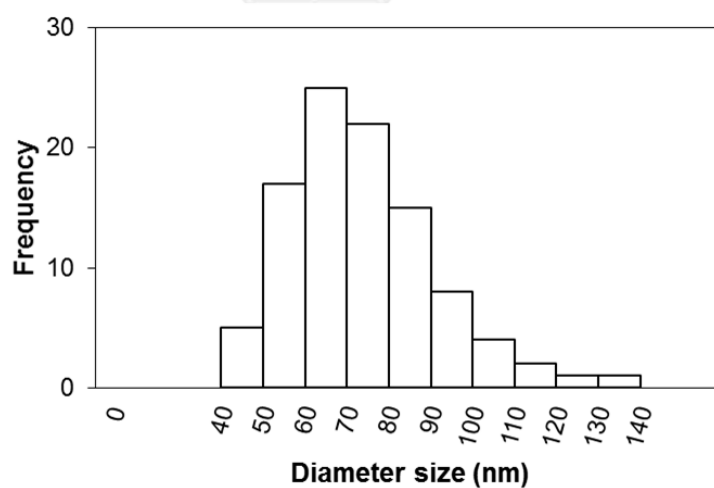


Figure 4.21 PSD of CNTs synthesized at 900°C

Meanwhile, with an increase in synthesizing temperature from 900 to 1000 °C the carbon spheres were produced with an average, minimum, maximum diameter size of 520, 320, 730 nm, respectively. Based on the morphology properties of carbon

spheres (**Figure 4.22**), the synthesizing temperature of 1000 °C could not be formed a CNTs.

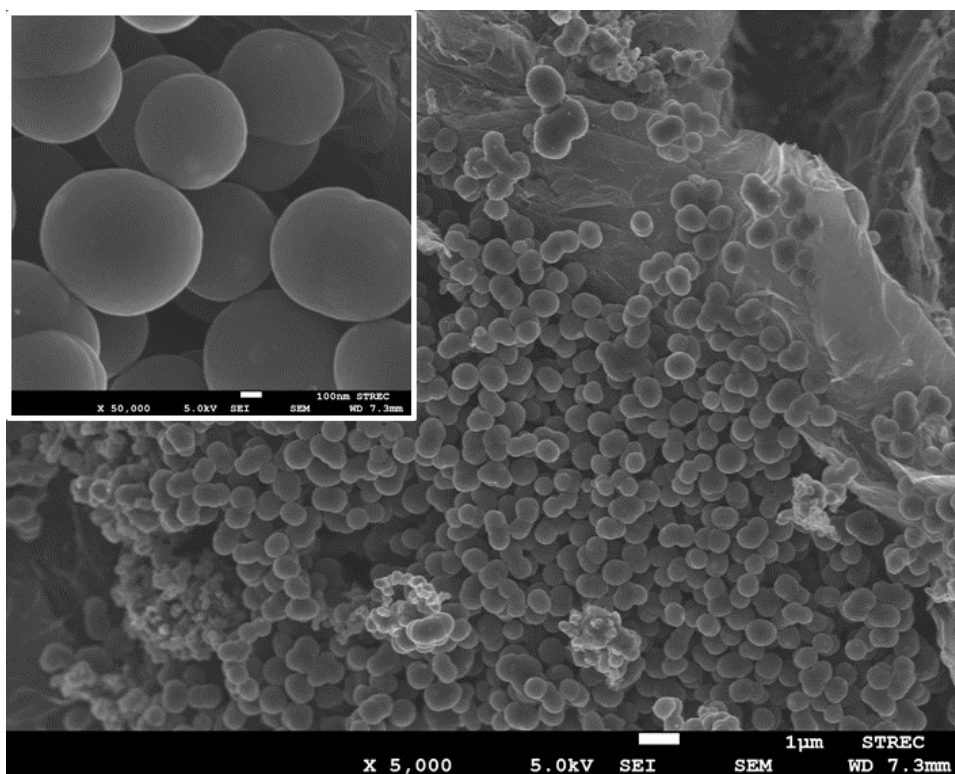


Figure 4.22 FESEM images of product synthesized at 1000°C

An increase in synthesizing temperature, the dissolving and diffusing rates of carbon atoms increase [3, 38]. The increase of the temperature lead to increase of a graphene layers in the CNT wall by accumulation of carbon atoms on outer surface of CNTs and increase of an inner diameters by larger catalyst size.

The Raman spectra (**Figure 4.23**) confirm the presence of both crystalline and non-crystalline carbon nanoparticles in the products which located at 1580 cm^{-1} (G band) and 1340 cm^{-1} (D band). Then the intensity ratio to G peak and D peak (I_G/I_D) indicate the degree of crystallinity of CNTs compared with amorphous. An increase in synthesizing temperature, I_G/I_D ratio of products synthesized at 700, 800, 900, and 1000 °C increase from 0.76, 1.45, 1.77, and 2.65, respectively. However, the morphology of

product synthesized at 1000 °C show the product in form of carbon sphere. In order to confirm the presence of crystalline CNTs within the products synthesized at 700, 800, and 900 °C, the highest ratio was obtained in synthesizing temperature of 900°C, showing the morphology of CNTs. In addition, the two characteristic peak located at ~ 1575 and 1590 cm^{-1} corresponding to the G band of CNTs and graphene, respectively [8]. From Raman spectra of product synthesized at 700°C, the peak located at $\sim 1590 \text{ cm}^{-1}$ can be assigned to the G band of graphene oxide. When synthesizing temperature increased to 800, 900, and 1000 °C, The G band slightly shifted to lower frequencies corresponded to G band from CNTs.

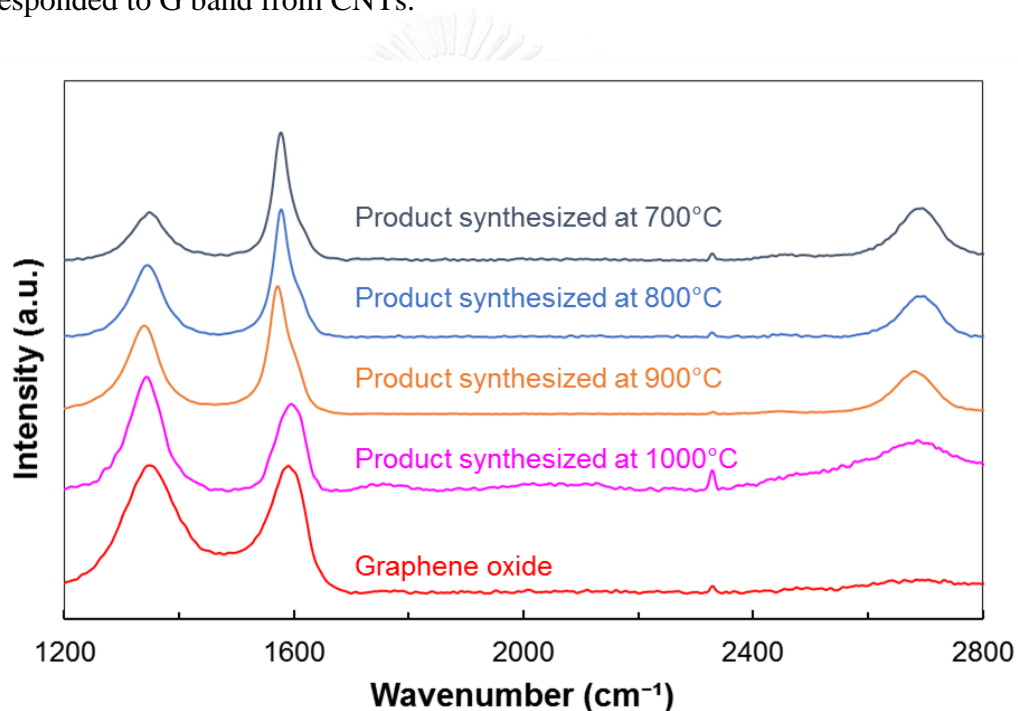


Figure 4.23 Raman spectra of GO and products synthesized at 700-1000 °C

BET analysis provides specific surface area (SSA), total pore volume and average pore diameter as shown in **Fig. 4.24** and **Table 4.3**. The total SSA and pore volume of CNT/G hybrid materials synthesized at 700°C reach $\sim 143 \text{ m}^2/\text{g}$ and $0.1949 \text{ cm}^3/\text{g}$, respectively. The total SSA value is increased from bare graphene oxide about 12 times. The total SSA is decreased significantly when the synthesizing temperature

increased from 700 to 800 and 900 °C. This value is decreased from 143 to 65 and 37 m²/g due to the density of CNTs on Fe/GO composite from morphological analysis. The density of iron oxide nanoparticles on Fe/GO treated at 700 °C is higher than Fe/GO treated at 800 and 900 °C. Therefore, the highest density of CNTs was obtained from synthesizing temperature of 700 °C. On the other hand, increases in total SSA and total pore volume correspond to a decrease in average pore diameter from 5.46 to 8.79 and 10.26 nm, respectively. When synthesizing temperature increased to 1000 °C, the total SSA is drastically decreased to 3 m²/g from 12 m²/g of bare graphene oxide.

Table 4.3 BET analysis of GO and CNT/G synthesized at 700-1000°C

	GO	CNT/G synthesized at various temperature			
		700°C	800°C	900°C	1000°C
a_{s,BET} (m ² /g)	11.948	142.70	64.656	37.281	2.9257
Total pore volume (cm ³ /g)	0.0033135	0.1949	0.1421	0.095609	0.010426
at p/p₀	0.952	0.953	0.951	0.953	0.954
Average pore diameter (nm)	1.1093	5.464	8.7917	10.258	14.255

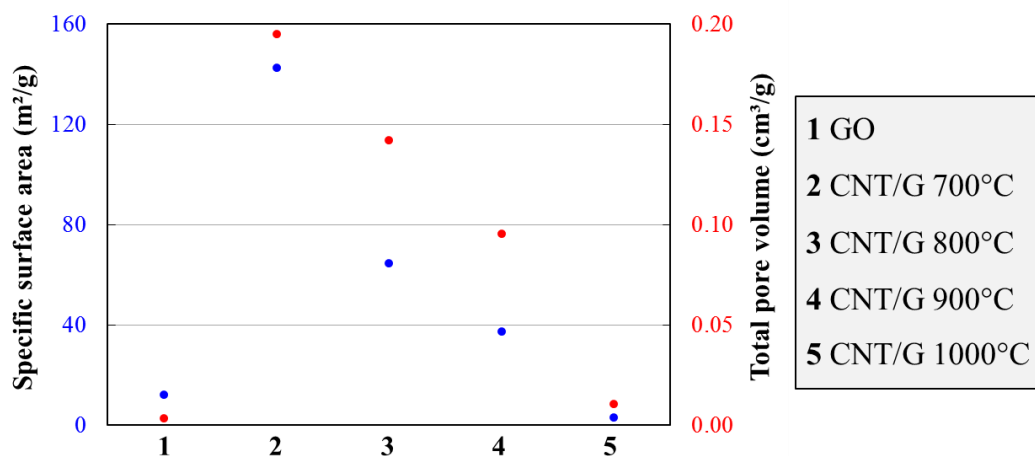


Figure 4.24 Relationship between SSA and total pore volume of GO and CNT/G synthesized at 700-1000 °C

Moreover, the influence of phase of iron catalyst on the formation of CNTs was investigated by CVD synthesis using Fe/GO composite, treated at 1000°C, in gamma-iron phase. The Fe/GO composite, treated at 900°C, shows the main diffraction peaks of alpha-iron phase. The both of iron oxide particles are average diameter of 98, and 119 nm. From previous research of Lee et al. [29] reported the average iron particle sizes of 90 and 150 nm can be formed the vertically aligned CNTs. The γ -Fe₂O₃, reduced before forming CNTs, generated the carbon-encapsulated iron nanoparticles. FESEM image (**Figure 4.25**) shows the formation of CNPs in forms of carbon-encapsulated iron nanoparticles, grown at synthesizing temperature of 900°C on Fe/GO composite treated at 1000°C. The effect of phase of iron on formation of CNTs was discussed that the alpha-iron implied formation of CNTs. Wirth et al. [52] reported the pathway of carbide formation from alpha-iron easier to obtain than gamma-iron due to carbide formation occurring with carbon nanotube formation. In comparison between product synthesized at 900 and 1000 °C on iron with gamma phase, the carbon atoms accumulated on the surface of iron catalyst to form a carbon-encapsulated iron

nanoparticles and carbon spheres, respectively. The wall thickness and outer diameters was increased due to high diffusion rate of carbon atoms at high temperature [53].

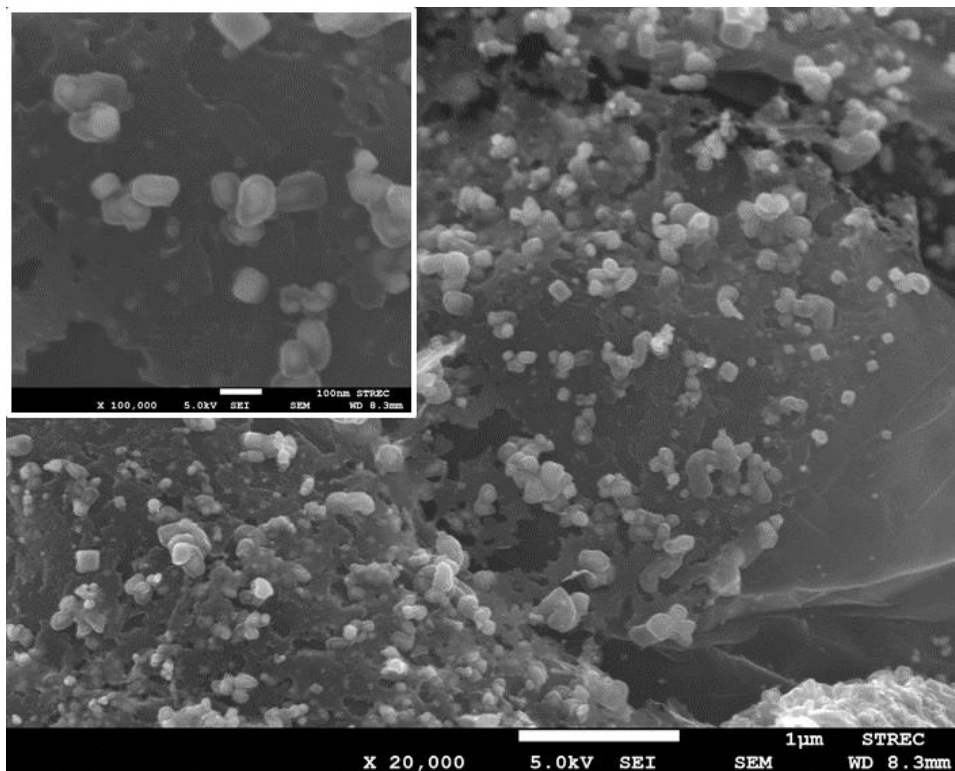


Figure 4.25 FESEM images of product synthesized at 900°C on Fe/GO composite treated at 1000°C

CHAPTER V

CONCLUSIONS AND RECOMMENDATIONS

5.1 Conclusions

In this research, the phenomena during synthesis of CNTs on Fe/GO composite catalyst via CVD of n-Hexane were investigated within the effect of synthesizing temperature on structural properties of Fe/GO composite catalyst, including crystal structures of an iron. In addition, the effect of crystal structures of an iron on formation of CNTs was also investigated. For obtaining the catalyst for synthesis of CNTs, Fe/GO composite was prepared by wet impregnation technique using iron(III)nitrate nonahydrate on graphene oxide prepared by modified Hummers method.

Based on our investigation, the iron oxide nanoparticles in Fe/GO composite catalyst were obtained with average particle size of 9 ± 3 nm from FESEM image and amorphous γ -Fe₂O₃ by XRD. During the CVD synthesis of CNTs, the particle size of iron oxide in Fe/GO composites was increased to 14 ± 5 , 72 ± 28 , 98 ± 37 , 119 ± 39 nm, when synthesizing temperature increased to 700, 800, 900, 1000 °C, respectively. After CVD of n-Hexane at temperature of 700, 800, and 900 °C, the synthesis obtained CNTs with diameter of 20-50, 20-80, and 50-100 nm, respectively. When synthesizing temperature increased to 1000 °C, the carbon spheres with diameter of 320-730 nm were obtained on the iron rich gamma phase in Fe/GO composite. In addition, degree of crystallinity of CNTs synthesized at 900 °C showed the I_G/I_D ratio of CNTs with 1.77 higher than synthesized at 700 °C (0.76) and 800 °C (1.45). The optimal synthesizing temperature for formation of CNTs was obtained at 900 °C.

The alpha iron completely transformed into gamma phase was occurred, when the synthesizing temperature increased to 1000 °C. The Fe/GO with gamma iron phase produced carbon-encapsulated iron nanoparticles and carbon spheres at synthesizing

temperature of 900 and 1000°C, respectively. The formation of CNTs essentially required the alpha iron phase.

5.2 Recommendations

1) The high reactivity to the oxidation of iron nanoparticles can be avoided by using in-situ X-ray Diffraction. To study the change in crystalline phase during CVD synthesis of CNTs without diffraction peaks corresponding to iron oxide.

2) To investigate effect of crystalline structures of an iron on CNTs formation, iron nanoparticles on graphene oxide were synthesized and controlled the particle size and particle size distribution.

3) In this present work, the pressure was fixed at atmospheric pressure. To investigate effect of pressure conditions, the pressure should be varied in vacuum pressure for improving rate of decomposition of carbon source and formation of CNTs.

4) The CNT/G hybrid materials should be characterized on improving electrical and physical properties in order to compare with bare graphene oxide and carbon nanotubes.

REFERENCES

- [1] W.Z. Li, S.S. Xie, L.X. Qian, B.H. Chang, B.S. Zou, W.Y. Zhou, R.A. Zhao, G. Wang, Large-Scale Synthesis of Aligned Carbon Nanotubes, *Science* 274 (1996) 1701-1703.
- [2] C.J. Lee, J. Park, J.A. Yu, Catalyst effect on carbon nanotubes synthesized by thermal chemical vapor deposition, *Chem. Phys. Lett.* 360(3-4) (2002) 250-255.
- [3] T. Charinpanitkul, N. Sano, P. Puengjinda, J. Klanwan, N. Akrapattangkul, W. Tanthapanichakoon, Naphthalene as an alternative carbon source for pyrolytic synthesis of carbon nanostructures, *J. Anal. Appl. Pyrolysis* 86(2) (2009) 386-390.
- [4] Á. Kukovecz, Z. Kónya, N. Nagaraju, I. Willems, A. Tamási, A. Fonseca, J.B. Nagy, I. Kiricsi, Catalytic synthesis of carbon nanotubes over Co, Fe and Ni containing conventional and sol-gel silica-aluminas, *Phys. Chem. Chem. Phys.* 2(13) (2000) 3071-3076.
- [5] P. Zarabadi-Poor, A. Badiei, A.A. Yousefi, B.D. Fahlman, A. Abbasi, Catalytic chemical vapour deposition of carbon nanotubes using Fe-doped alumina catalysts, *Catal. Today* 150(1-2) (2010) 100-106.
- [6] M. Kumar, Y. Ando, Chemical Vapor Deposition of Carbon Nanotubes: A Review on Growth Mechanism and Mass Production, *J. Nanosci. Nanotechnol.* 10(6) (2010) 3739-3758.
- [7] K.A. Shah, B.A. Tali, Synthesis of carbon nanotubes by catalytic chemical vapour deposition: A review on carbon sources, catalysts and substrates, *Mater. Sci. Semicond. Process.* 41 (2016) 67-82.
- [8] X. Dong, B. Li, A. Wei, X. Cao, M.B. Chan-Park, H. Zhang, L.-J. Li, W. Huang, P. Chen, One-step growth of graphene-carbon nanotube hybrid materials by chemical vapor deposition, *Carbon* 49(9) (2011) 2944-2949.
- [9] Z. Fan, J. Yan, L. Zhi, Q. Zhang, T. Wei, J. Feng, M. Zhang, W. Qian, F. Wei, A three-dimensional carbon nanotube/graphene sandwich and its application as electrode in supercapacitors, *Adv. Mater.* 22(33) (2010) 3723-3728.
- [10] Y. Zhu, L. Li, C. Zhang, G. Casillas, Z. Sun, Z. Yan, G. Ruan, Z. Peng, A.-R.O. Raji, C. Kittrell, R.H. Hauge, J.M. Tour, A seamless three-dimensional carbon nanotube graphene hybrid material, *Nat. Commun.* 3 (2012).
- [11] M.-Y. Yen, M.-C. Hsiao, S.-H. Liao, P.-I. Liu, H.-M. Tsai, C.-C.M. Ma, N.-W. Pu, M.-D. Ger, Preparation of graphene/multi-walled carbon nanotube hybrid and its use as photoanodes of dye-sensitized solar cells, *Carbon* 49(11) (2011) 3597-3606.
- [12] T.G. Digges, S.J. Rosemberg, Metallographic study of the formation of austenite from aggregates of ferrite and cementite in an iron-carbon alloy of 0.5 percent carbon, *Bur. Stand. J. Res.* 29(2) (1942) 113-121.

- [13] J.L. Dossett, H.E. Boyer, *Practical Heat Treating*, Second ed., ASM International, Materials Park, OH, USA, 2006.
- [14] Z. Xiong, L.L. Zhang, J. Ma, X.S. Zhao, Photocatalytic degradation of dyes over graphene-gold nanocomposites under visible light irradiation, *Chem. Commun.* 46(33) (2010) 6099-6101.
- [15] J. Zhang, H. Yang, G. Shen, P. Cheng, J. Zhang, S. Guo, Reduction of graphene oxide via L-ascorbic acid, *Chem. Commun.* 46(7) (2010) 1112-1114.
- [16] A.K. Fard, T. Rhadfi, G. McKay, M. Al-marri, A. Abdala, N. Hilal, M.A. Hussien, Enhancing oil removal from water using ferric oxide nanoparticles doped carbon nanotubes adsorbents, *Chem. Eng. J.* 293 (2016) 90-101.
- [17] A. Reina, X. Jia, J. Ho, D. Nezich, H. Son, V. Bulovic, M.S. Dresselhaus, J. Kong, Large Area, Few-Layer Graphene Films on Arbitrary Substrates by Chemical Vapor Deposition, *Nano letters* 9(1) (2009) 30-35.
- [18] K.S. Novoselov, A.K. Geim, S.V. Morozov, D. Jiang, Y. Zhang, S.V. Dubonos, I.V. Grigorieva, A.A. Firsov, Electric Field Effect in Atomically Thin Carbon Films, *Science* 306(5696) (2004) 666-669.
- [19] H.W. Kroto, J.R. Heath, S.C. O'Brien, R.F. Curl, R.E. Smalley, C60: Buckminsterfullerene, *Nature* 318(6042) (1985) 162-163.
- [20] S. Iijima, M. Yudasaka, R. Yamada, S. Bandow, K. Suenaga, F. Kokai, K. Takahashi, Nano-aggregates of single-walled graphitic carbon nano-horns, *Chem. Phys. Lett.* 309(3-4) (1999) 165-170.
- [21] S. Iijima, Helical microtubules of graphitic carbon, *Nature* 354 (1991) 56-58.
- [22] S. Park, R.S. Ruoff, Chemical methods for the production of graphenes, *Nat. Nanotechnol.* 4 (2009) 217-224.
- [23] W.S. Hummers, R.E. Offeman, Preparation of Graphitic Oxide, *J. Am. Chem. Soc.* 80(6) (1958) 1339.
- [24] O.C. Compton, S.T. Nguyen, Graphene oxide, highly reduced graphene oxide, and graphene: versatile building blocks for carbon-based materials, *Small* 6(6) (2010) 711-723.
- [25] S.Y. Madani, A. Mandel, A.M. Seifalian, A concise review of carbon nanotube's toxicology, *Nano Rev.* 4 (2013).
- [26] B.C. Brodie, On the Atomic Weight of Graphite, *Phil. Trans. R. Soc. Lond.* 149 (1859) 249-259.
- [27] L. Staudenmaier, Verfahren zur Darstellung der Graphitsäure, *L. Ber. Dtsch. Chem. Ges.* 31(2) (1898) 1481-1487.
- [28] F.N. Sayed, V. Polshettiwar, Facile and sustainable synthesis of shaped iron oxide nanoparticles: effect of iron precursor salts on the shapes of iron oxides, *Sci. Rep.* 5 (2015) 1-14.
- [29] C.J. Lee, J. Park, Y. Huh, J.Y. Lee, Temperature effect on the growth of carbon nanotubes using thermal chemical vapor deposition, *Chem. Phys. Lett.* 343(1-2) (2001) 33-38.

- [30] J.-H. Kim, K.H. Lee, D. Burk, L.J. Overzet, G.S. Lee, The effects of pre-annealing in either H₂ or He on the formation of Fe nanoparticles for growing spin-capable carbon nanotube forests, *Carbon* 48(15) (2010) 4301-4308.
- [31] D. Wang, Y. Li, Q. Wang, T. Wang, Nanostructured Fe₂O₃-graphene composite as a novel electrode material for supercapacitors, *J. Solid State Electrochem.* 16(6) (2011) 2095-2102.
- [32] S. Sarkar, A. Mondal, K. Dey, R. Ray, Magnetic memory in nanocrystalline α -Fe₂O₃ embedded in reduced graphene oxide, *RSC Adv.* 5(99) (2015) 81260-81265.
- [33] X. Li, L. Ai, J. Jiang, Nanoscale zerovalent iron decorated on graphene nanosheets for Cr(VI) removal from aqueous solution: Surface corrosion retard induced the enhanced performance, *Chem. Eng. J.* 288 (2016) 789-797.
- [34] H.A. Asmaly, B. Abussaud, Ihsanullah, T.A. Saleh, V.K. Gupta, M.A. Atieh, Ferric oxide nanoparticles decorated carbon nanotubes and carbon nanofibers: From synthesis to enhanced removal of phenol, *J. Saudi Chem. Soc.* 19(5) (2015) 511-520.
- [35] S. Yuvaraj, L. Fan-Yuan, C. Tsong-Huei, Y. Chuin-Tih, Thermal Decomposition of Metal Nitrates in Air and Hydrogen Environments, *J. Phys. Chem. B* 107(4) (2003) 1044-1047.
- [36] N. Mishra, G. Das, A. Ansaldo, A. Genovese, M. Malerba, M. Povia, D. Ricci, E.D. Fabrizio, E.D. Zitti, M. Sharon, M. Sharon, Pyrolysis of waste polypropylene for the synthesis of carbon nanotubes, *J. Anal. Appl. Pyrolysis* 94 (2012) 91-98.
- [37] Y. Li, H. Wang, G. Wang, J. Gao, Synthesis of single-walled carbon nanotubes from heavy oil residue, *Chem. Eng. J.* 211-212 (2012) 255-259.
- [38] P. Puengjinda, N. Sano, W. Tanthapanichakoon, T. Charinpanitkul, Selective synthesis of carbon nanotubes and nanocapsules using naphthalene pyrolysis assisted with ferrocene, *J. Ind. Eng. Chem.* 15(3) (2009) 375-380.
- [39] S.-P. Chai, S.H.S. Zein, A.R. Mohamed, Preparation of carbon nanotubes over cobalt-containing catalysts via catalytic decomposition of methane, *Chem. Phys. Lett.* 426(4-6) (2006) 345-350.
- [40] V.C. Tung, L.-M. Chen, M.J. Allen, J.K. Wassei, K. Nelson, R.B. Kaner, Y. Yang, Low-Temperature Solution Processing of Graphene–Carbon Nanotube Hybrid Materials for High-Performance Transparent Conductors, *Nano Lett.* 9(5) (2009) 1949-1955.
- [41] P. Mandal, A.P. Chattopadhyay, Excellent catalytic activity of magnetically recoverable Fe₃O₄-graphene oxide nanocomposites prepared by a simple method, *Dalton Trans.* 44(25) (2015) 11444-11456.
- [42] M. Hirata, T. Gotou, S. Horiuchi, M. Fujiwara, M. Ohba, Thin-film particles of graphite oxide 1: High-yield synthesis and flexibility of the particles, *Carbon* 42(14) (2004) 2929-2937.
- [43] S.H. Huh, Physics and Applications of Graphene - Experiments, Thermal Reduction of Graphene Oxide, InTech2011.

- [44] H. Su, Z. Ye, N. Hmidi, High-performance iron oxide-graphene oxide nanocomposite adsorbents for arsenic removal, *Colloids Surf., A* 522 (2017) 161-172.
- [45] D.K. Bora, A. Braun, S. Erat, O. Safonova, T. Graule, E.C. Constable, Evolution of structural properties of iron oxide nano particles during temperature treatment from 250°C-900°C: X-ray diffraction and Fe K-shell pre-edge X-ray absorption study, *Curr. Appl. Phys.* 12(3) (2012) 817-825.
- [46] R. Sun, H.-B. Zhang, J. Yao, D. Yang, Y.-W. Mai, Z.-Z. Yu, In situ reduction of iron oxide with graphene for convenient synthesis of various graphene hybrids, *Carbon* 107 (2016) 138-145.
- [47] R.L. Penn, J.A. Soltis, Characterizing crystal growth by oriented aggregation, *CrystEngComm* 16(8) (2014) 1409-1418.
- [48] M. Aronniemi, J. Lahtinen, P. Hautojärvi, Characterization of iron oxide thin films, *Surf. Interface Anal.* 36(8) (2004) 1004-1006.
- [49] X. Zhan, H. Tang, Y. Du, A. Talbi, J. Zha, J. He, Facile preparation of Fe nanochains and their electromagnetic properties, *RSC Adv.* 3(36) (2013) 15966-15970.
- [50] M.-C. Chou, C.-F. Chu, S.-T. Wu, Phase transformations of electroplated amorphous iron-tungsten-carbon film, *Mater. Chem. Phys.* 78(1) (2003) 59-66.
- [51] H. Niu, J. Lu, J. Song, L. Pan, X. Zhang, L. Wang, J.-J. Zou, Iron Oxide as a Catalyst for Nitroarene Hydrogenation: Important Role of Oxygen Vacancies, *Ind. Eng. Chem. Res.* 55(31) (2016) 8527-8533.
- [52] C.T. Wirth, B.C. Bayer, A.D. Gamalski, S. Esconjauregui, R.S. Weatherup, C. Ducati, C. Baehtz, J. Robertson, S. Hofmann, The Phase of Iron Catalyst Nanoparticles during Carbon Nanotube Growth, *Chem. Mater.* 24(24) (2012) 4633-4640.
- [53] W.Z. Li, J.G. Wen, Z.F. Ren, Effect of temperature on growth and structure of carbon nanotubes by chemical vapor deposition, *Applied Physics A* 74(3) (2002) 397-402.

APPENDIX



จุฬาลงกรณ์มหาวิทยาลัย
CHULALONGKORN UNIVERSITY

APPENDIX A

Table A1 Iron oxide particle size of as-prepared Fe/GO composite and Fe/GO composites treated at temperature of 700-1000 °C

Counts	As-prepared	700°C	800°C	900°C	1000°C
1	3.2	5.3	24.1	40.9	55.7
2	3.5	5.9	25.4	41.4	56.7
3	4.4	5.9	28.6	44.1	57.0
4	4.7	6.6	28.8	45.4	59.6
5	5.1	6.6	31.7	46.0	63.5
6	5.4	7.1	31.7	50.2	64.2
7	5.7	7.5	32.2	51.4	64.7
8	5.7	7.6	32.7	51.7	67.5
9	5.7	7.7	34.6	54.4	71.5
10	5.8	7.9	35.5	56.5	74.0
11	5.8	8.1	36.6	58.1	75.3
12	5.8	8.8	39.3	59.9	76.4
13	6.1	8.9	39.5	61.5	78.8
14	6.2	9.2	39.5	63.4	78.8
15	6.3	9.4	39.8	64.0	79.7
16	6.5	9.7	39.8	65.1	80.1
17	6.5	9.7	40.8	65.3	80.4
18	6.6	10.2	43.0	65.3	80.7
19	6.6	10.2	43.0	66.3	80.7
20	6.7	10.3	43.0	67.7	81.5
21	6.8	10.7	43.8	68.1	84.3
22	6.8	10.7	44.2	69.7	86.1
23	6.8	10.7	44.3	71.2	86.9
24	6.9	10.7	49.7	71.9	88.1
25	6.9	11.3	50.0	72.1	88.7
26	7.2	11.3	51.2	72.5	90.0
27	7.2	11.3	51.5	74.0	92.4
28	7.2	11.4	51.6	75.0	94.3
29	7.3	11.4	52.9	75.4	94.7
30	7.3	11.7	53.1	75.5	95.6
31	7.3	11.8	57.2	76.1	95.6
32	7.3	11.8	58.9	77.2	97.0
33	7.4	12.1	60.0	77.9	97.9
34	7.4	12.4	60.0	78.4	98.3

Counts	As-prepared	700°C	800°C	900°C	1000°C
35	7.4	12.4	60.8	78.5	98.9
36	7.5	12.4	60.8	79.1	100.5
37	7.5	12.4	60.9	79.8	103.1
38	7.5	12.4	61.2	80.7	105.5
39	7.6	12.6	61.2	81.5	106.3
40	7.6	12.6	64.4	83.7	107.0
41	7.6	12.9	64.5	83.9	108.1
42	8.1	13.0	65.9	84.1	108.4
43	8.4	13.4	66.5	84.5	109.0
44	8.6	13.5	67.5	84.5	110.3
45	8.6	14.0	67.8	87.7	110.3
46	8.7	14.0	68.0	87.8	112.4
47	8.9	14.2	68.3	88.1	112.9
48	8.9	14.2	69.4	88.8	113.6
49	8.9	14.5	71.5	92.6	114.2
50	8.9	14.8	71.6	93.4	115.3
51	8.9	14.8	71.6	93.9	115.3
52	9.0	14.8	71.8	94.1	117.6
53	9.0	15.1	71.8	94.2	119.2
54	9.0	15.1	71.9	94.3	119.6
55	9.1	15.4	75.1	96.1	120.0
56	9.1	15.4	75.1	96.3	120.1
57	9.1	15.6	75.4	98.7	121.6
58	9.4	15.6	75.8	99.0	121.8
59	9.4	16.0	77.2	99.0	121.9
60	9.5	16.0	79.7	99.6	122.4
61	9.5	16.0	80.9	100.3	122.5
62	9.5	16.1	80.9	101.5	122.9
63	9.6	16.1	81.5	101.8	124.8
64	9.6	16.1	82.3	101.9	125.3
65	9.8	16.2	82.3	103.7	125.7
66	9.9	16.7	82.5	105.3	127.0
67	10.0	16.7	82.9	107.2	129.1
68	10.0	16.7	83.7	108.0	129.8
69	10.1	17.1	85.0	108.1	130.1
70	10.3	17.2	85.8	108.8	132.7
71	10.3	17.2	85.9	109.5	133.3
72	10.4	17.7	87.5	110.5	133.8
73	10.6	17.8	88.3	111.2	139.5
74	10.8	17.8	89.6	111.5	139.5

Counts	As-prepared	700°C	800°C	900°C	1000°C
75	11.1	17.8	89.6	112.1	140.8
76	11.2	17.8	90.2	116.4	141.6
77	11.2	17.9	90.6	117.9	141.6
78	11.2	18.3	91.1	120.8	143.0
79	11.3	18.3	91.2	122.0	143.3
80	11.4	18.4	91.3	123.8	143.6
81	11.8	18.4	92.8	125.5	144.2
82	11.8	19.0	93.5	128.5	144.5
83	11.8	19.0	95.9	130.9	144.8
84	11.8	19.3	96.6	132.4	149.1
85	11.9	19.4	97.2	135.0	153.2
86	12.3	19.5	97.6	138.0	157.3
87	12.5	19.6	97.6	140.6	161.0
88	12.6	20.2	100.7	142.6	161.9
89	12.6	20.2	101.1	145.3	162.4
90	12.6	20.2	103.3	151.4	166.3
91	12.9	20.3	108.9	153.5	168.6
92	13.2	20.7	109.1	154.3	180.0
93	13.4	20.7	114.4	154.9	185.2
94	14.0	20.9	114.4	163.1	193.7
95	14.0	21.5	115.3	163.9	196.6
96	14.1	21.5	124.3	165.9	201.9
97	14.2	22.0	124.4	186.1	202.4
98	14.8	22.3	129.1	190.5	212.1
99	14.8	24.2	153.9	198.5	216.4
100	14.8	25.8	156.2	227.8	243.5

Table A2 Statistical analysis of iron oxide particle size in as-prepared Fe/GO composite and Fe/GO composites treated at temperature of 700-1000 °C

	As-prepared	700°C	800°C	900°C	1000°C
Avg	9	14	72	98	119
Max	15	26	156	228	244
Min	3	5	24	41	56
StdDev	3	5	28	37	39

Appendix B

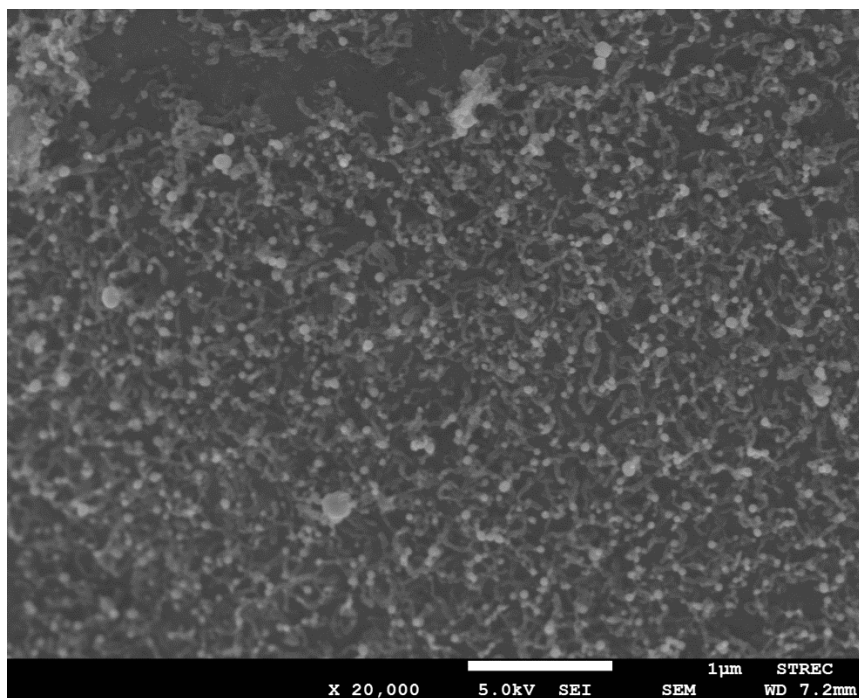


Figure B1 FESEM image of product synthesized at 700°C with magnification of 20,000X

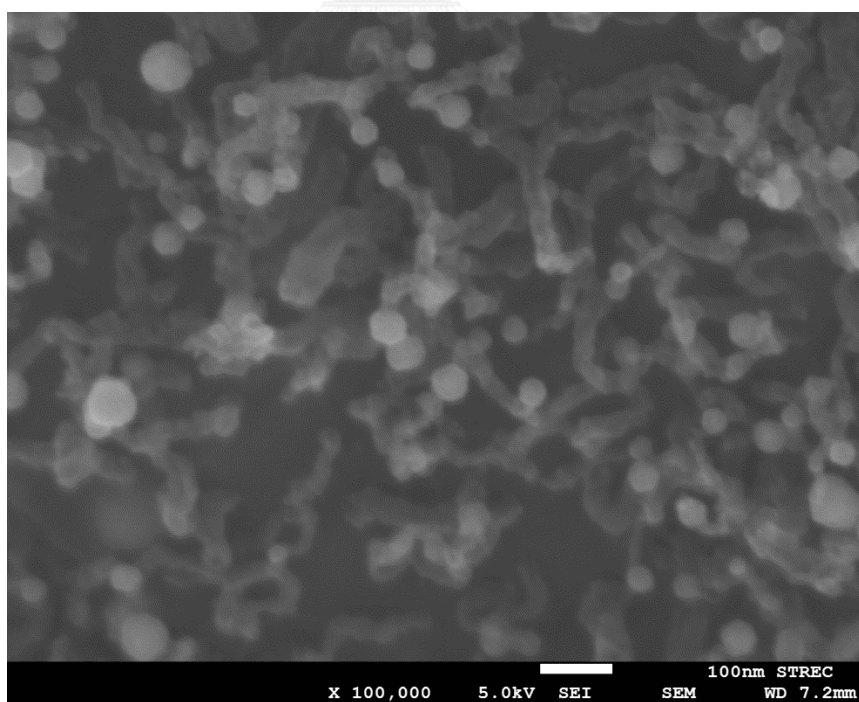


Figure B2 FESEM image of product synthesized at 700°C with magnification of 100,000X

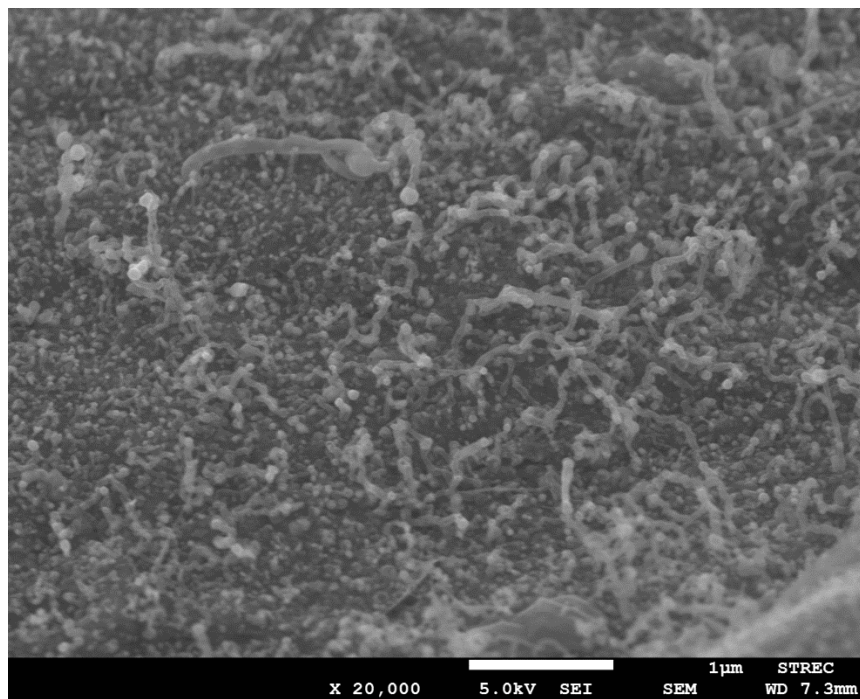


Figure B3 FESEM image of product synthesized at 800°C with magnification of 20,000X

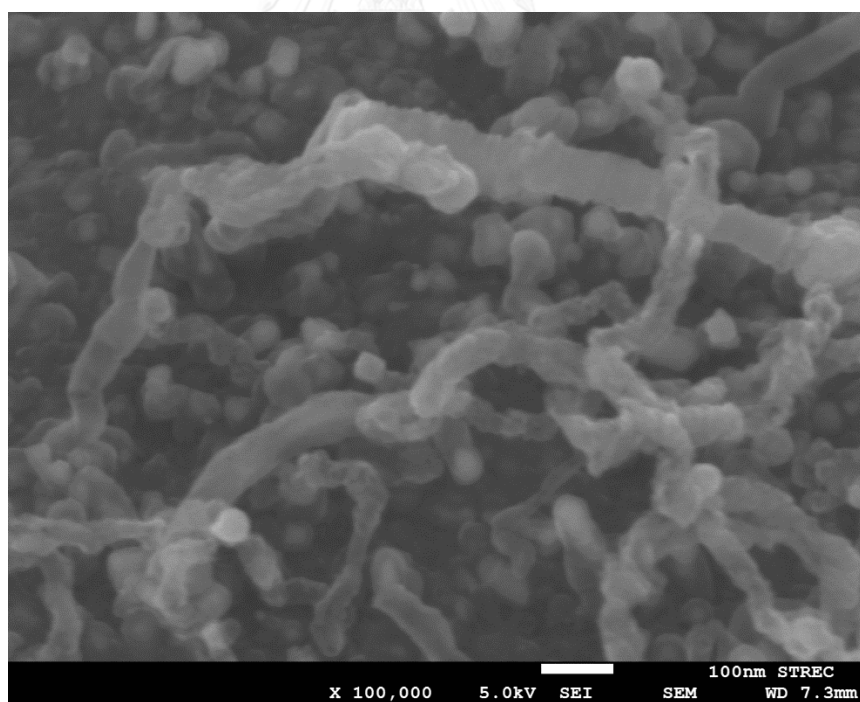


Figure B4 FESEM image of product synthesized at 800°C with magnification of 100,000X

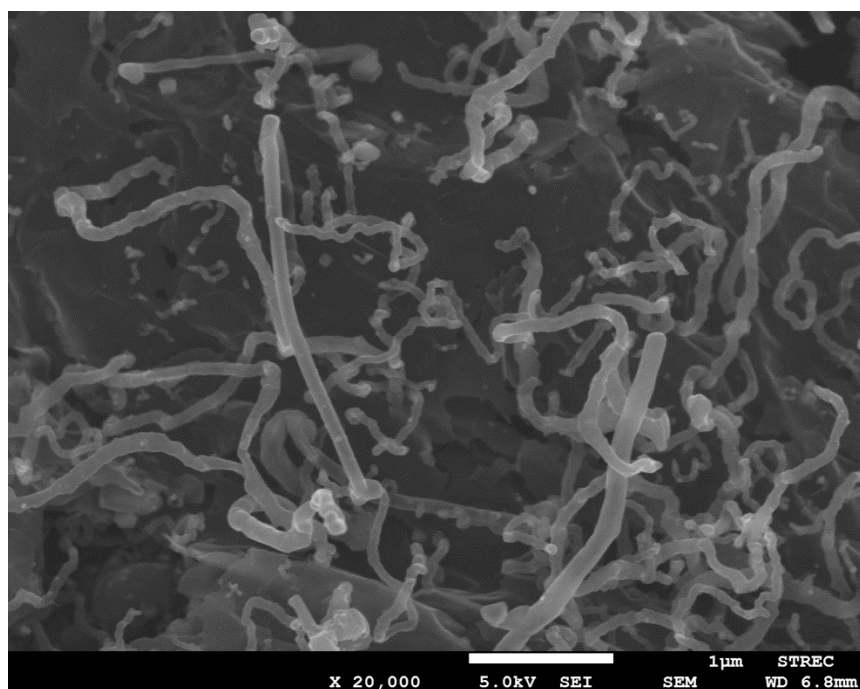


Figure B5 FESEM image of product synthesized at 900°C with magnification of 20,000X

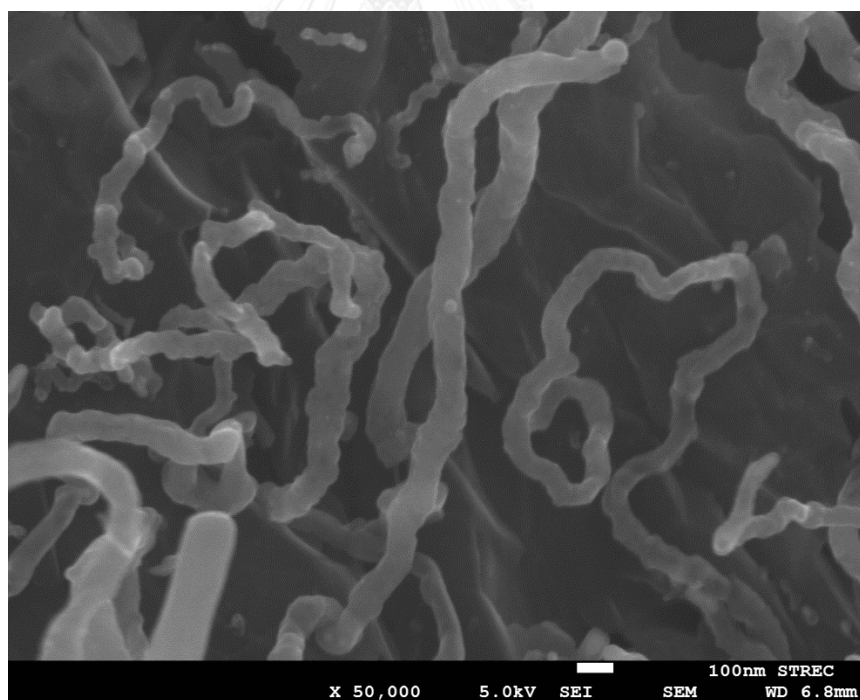


Figure B6 FESEM image of product synthesized at 900°C with magnification of 100,000X

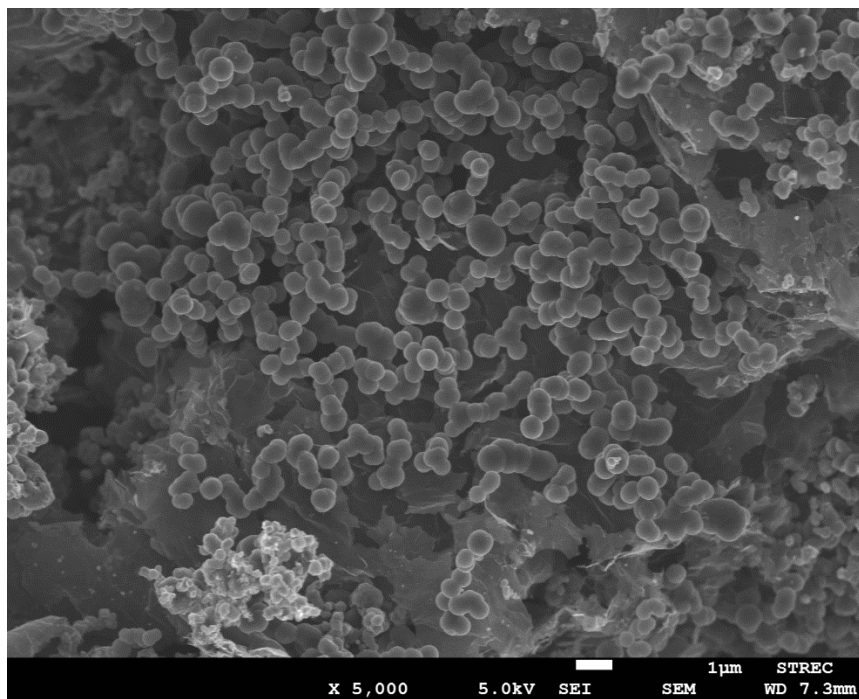


Figure B7 FESEM image of product synthesized at 1000°C with magnification of 5,000X

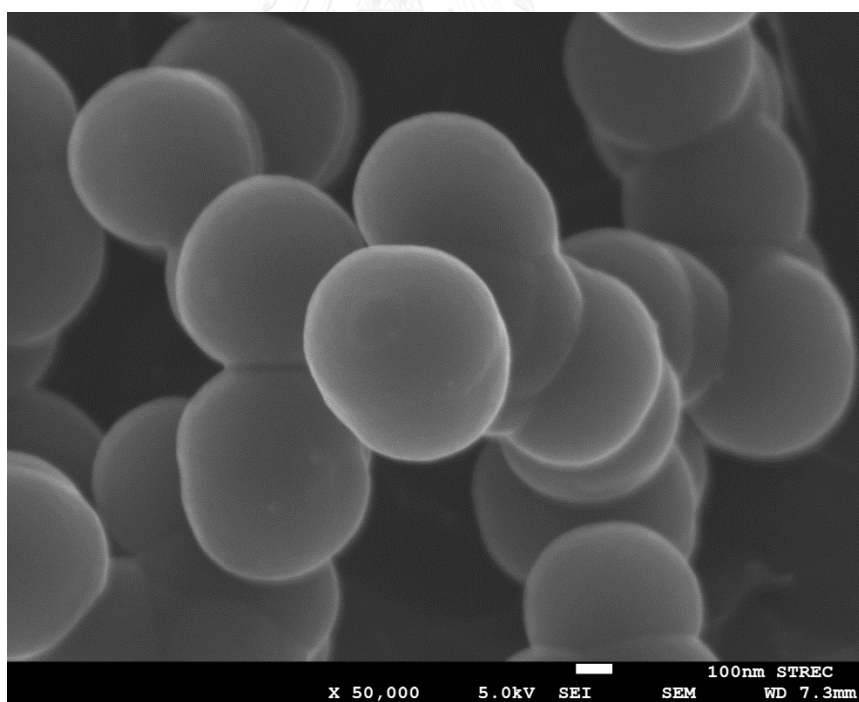


Figure B8 FESEM image of product synthesized at 1000°C with magnification of 50,000X

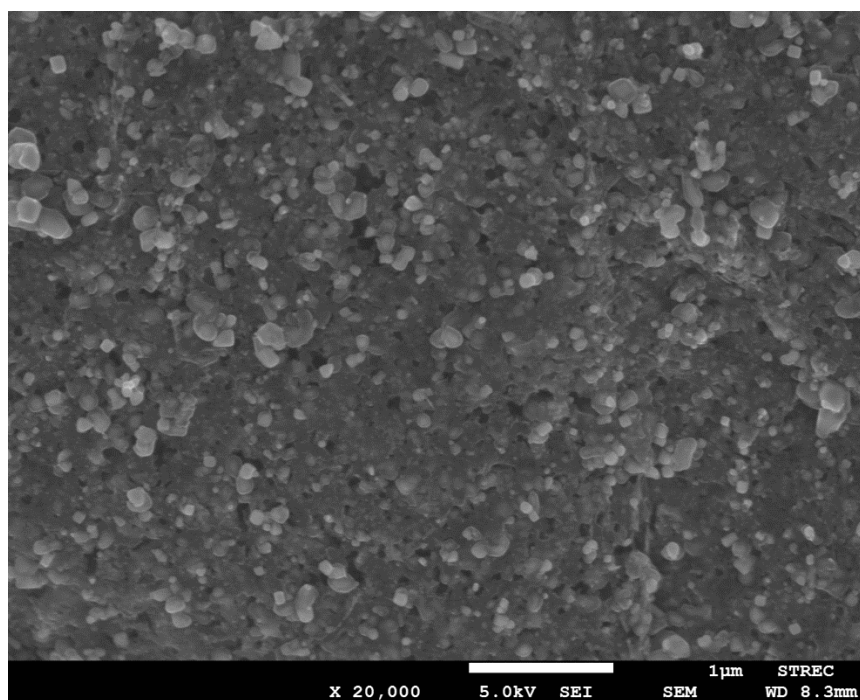


Figure B9 FESEM image of product synthesized at 900°C on Fe/GO treated at 1000°C with magnification of 20,000X

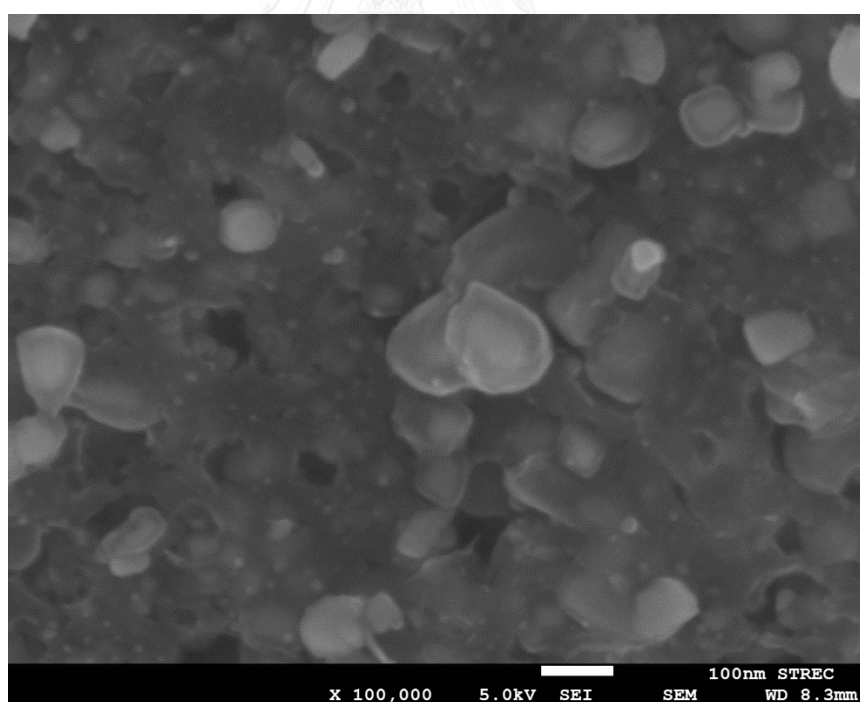


Figure B10 FESEM image of product synthesized at 900°C on Fe/GO treated at 1000°C with magnification of 100,000X

VITA

Mr. Oukrit Thonganuntakul was born in Bangkok, Thailand, on August 8, 1991. He attended at Debsirin school, Bangkok for high school. In 2014, he graduated Bachelor degree of Engineering in Chemical Engineering from Mahidol University, Nakhon Pathom. After that, he continued to study in Master degree in Center of Excellence in Particle Technology at Department of Chemical Engineering, Faculty of Engineering, Chulalongkorn University. During the period of his study in the degree of Master, he involved the research and development of PTT Research and Technology Institute (PTT RTI) for 1 and a half years as a research assistant.

